Journal of Medicinal Chemistry

pubs.acs.org/jmc

Article

A Small-Molecule Oral Agonist of the Human Glucagon-like Peptide-1 Receptor

David A. Griffith,* David J. Edmonds, Jean-Philippe Fortin, Amit S. Kalgutkar, J. Brent Kuzmiski, Paula M. Loria, Aditi R. Saxena, Scott W. Bagley, Clare Buckeridge, John M. Curto, David R. Derksen, João M. Dias, Matthew C. Griffor, Seungil Han, V. Margaret Jackson, Margaret S. Landis, Daniel Lettiere, Chris Limberakis, Yuhang Liu, Alan M. Mathiowetz, Jayesh C. Patel, David W. Piotrowski, David A. Price, Roger B. Ruggeri, and David A. Tess

Cite This: *J. Med. Chem.* 2022, 65, 8208−8226

Read Online

ACCESS | Metrics & More | Article Recommendations | Supporting Information

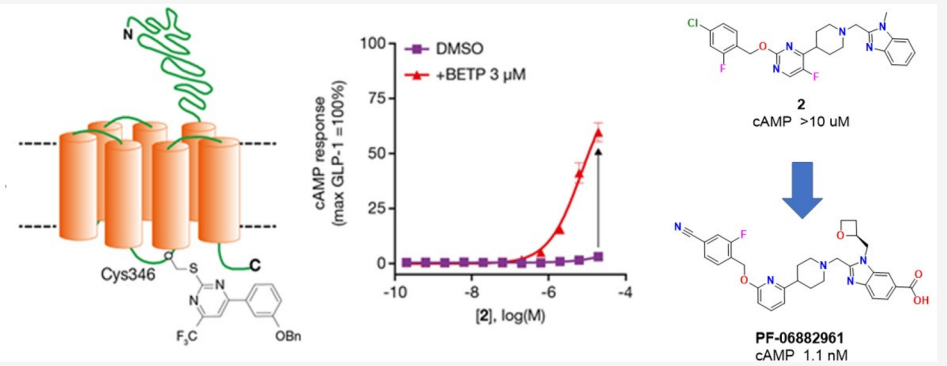

ABSTRACT: Peptide agonists of the glucagon-like peptide-1 receptor (GLP-1R) have revolutionized diabetes therapy, but their use has been limited because they require injection. Herein, we describe the discovery of the orally bioavailable, small-molecule, GLP-1R agonist PF-06882961 (danuglipron). A sensitized high-throughput screen was used to identify 5-fluoropyrimidine-based GLP-1R agonists that were optimized to promote endogenous GLP-1R signaling with nanomolar potency. Incorporation of a carboxylic acid moiety provided considerable GLP-1R potency gains with improved off-target pharmacology and reduced metabolic clearance, ultimately resulting in the identification of danuglipron. Danuglipron increased insulin levels in primates but not rodents, which was explained by receptor mutagensis studies and a cryogenic electron microscope structure that revealed a binding pocket requiring a primate-specific tryptophan 33 residue. Oral administration of danuglipron to healthy humans produced dose-proportional increases in systemic exposure (NCT03309241). This opens an opportunity for oral small-molecule therapies that target the well-validated GLP-1R for metabolic health.

INTRODUCTION

Glucagon-like peptide-1 (GLP-1), a neuroendocrine hormone, is derived from a proglucagon precursor[1] and secreted by intestinal enteroendocrine L cells in response to nutrient intake,[2] predominantly in the form of GLP-1(7−36) amide (henceforth GLP-1).[3] Activation of the GLP-1 receptor (GLP-1R) by GLP-1 stimulates insulin release and inhibits glucagon secretion in a glucose-dependent manner.[4] Also, GLP-1R agonism delays gastric emptying,[5] increases satiety, suppresses food intake, and reduces weight in humans.[6,7] Multiple injectable peptidic GLP-1R agonists are approved for the treatment of type 2 diabetes mellitus (T2DM),[8] including liraglutide and semaglutide,[9] which are also approved for the treatment of obesity.[10] Excitement has grown in this drug class, with several GLP-1R agonists demonstrating benefit in cardiovascular outcome studies.[11] A drawback of these medicines has been the necessity to administer them via subcutaneous injection, which limits patient utilization and may reduce opportunities for fixed dose combination treatments with other small-molecule therapies for cardio-metabolic diseases. Importantly, patients prefer, and are more likely to adhere to, an oral drug regimen versus an injectable alternative.[12] An orally administered formulation of the peptidic GLP-1R agonist semaglutide was recently approved

Received: October 28, 2021
Published: June 1, 2022

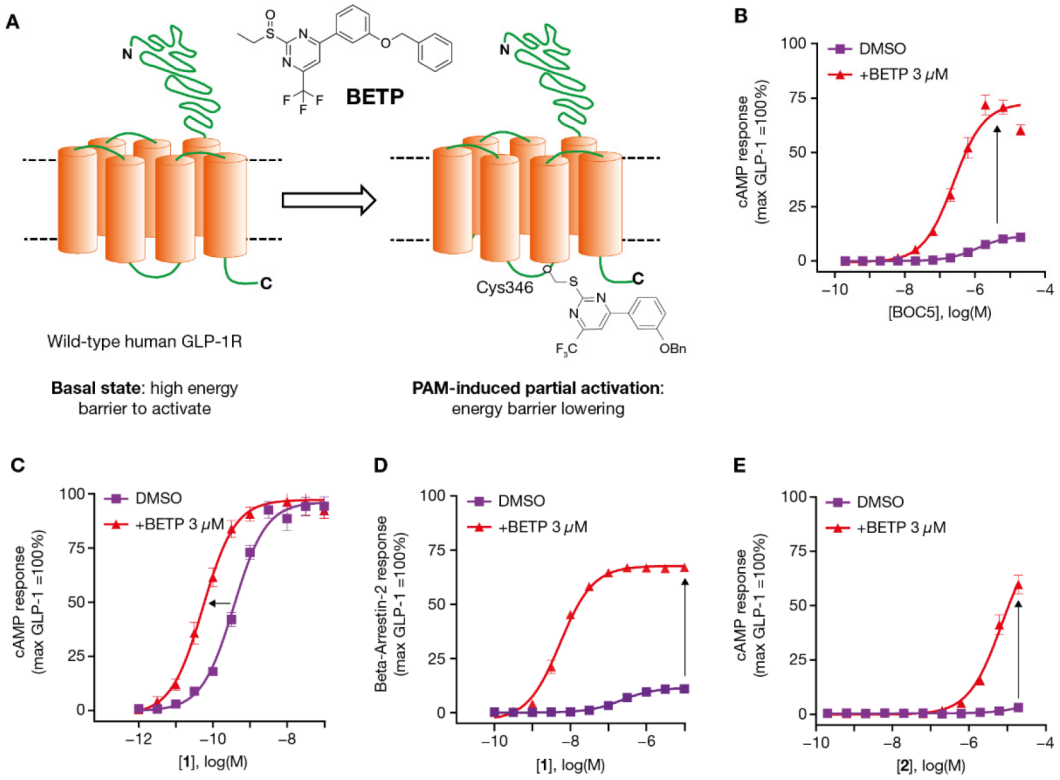

Figure 1. Identification of small-molecule GLP-1R agonists in a CHO-GLP-1R cellular assay in the absence or presence of the positive allosteric modulator BETP. (A) Assay concept. Covalent modification of Cys347 in the GLP-1R by BETP lowers the receptor activation barrier,[27] enabling the identification of weak agonists. (B–D) Validation of the BETP-sensitized screening assay. (B) BETP potentiates agonist-induced cAMP production of a small molecule (Boc-5) (Figure 2). (C and D) BETP potentiates cAMP production and β-arrestin recruitment, respectively, by peptide **1** (Figure 2) at the human GLP-1R. (E) cAMP curves of a representative small-molecule HTS hit, compound **2** (Figure 2). cAMP data normalized using 100 nM (+BETP) or 1 μM (+DMSO) GLP-1 response (100%), β-arrestin recruitment data normalized using 1 μM GLP-1 (100%). Data represent the mean ± the standard error of the mean (SEM) from two (B, DMSO), three (C and D, BETP), four (C and D, DMSO), six (B, BETP), seven (E, DMSO), or eight (E, BETP) experiments, each performed in duplicate; error bars are within the displayed symbols. Abbreviations: BETP, 4-[3-(benzyloxy)phenyl]-2-ethylsulfinyl-6-(trifluoromethyl)pyrimidine; cAMP, cyclic adenosine monophosphate; CHO, Chinese hamster ovary; DMSO, dimethyl sulfoxide; GLP-1R, glucagon-like peptide-1 receptor; PAM, positive allosteric modulator.

for the treatment of T2DM.[13] This peptidic drug is co-formulated with sodium *N*-[8-(2-hydroxybenzoyl)amino]-caprylate, a gastric absorption enhancer, to promote oral bioavailability. The dosage must be taken once daily in a fasted state with minimal liquid and at a dose substantially larger than that of the approved once-weekly injectable formulation.[13,14] In contrast, the GLP-1R agonists disclosed herein are traditional small molecules that are orally bioavailable in standard formulations (e.g., methylcellulose) and have the potential to be combined with other oral small-molecule therapeutics.

The GLP-1R is a seven-transmembrane-spanning, class B, G protein-coupled receptor (GPCR).[15] Class B GPCRs, including the GLP-1R, are activated by endogenous peptide hormones, and the development of small-molecule agonists of these receptors has proven to be particularly challenging.[15] Significant prior efforts across the pharmaceutical industry have generally failed to identify potent and efficacious small-molecule agonists of the GLP-1R,[16,17] although a recent report has revealed the identification of a potent, nonpeptidic orally active agonist series (exemplified by LY3502970), which is structurally distinct from danuglipron.[18] Given the significant therapeutic value of this mechanism, we pursued a novel high-throughput screening (HTS) strategy that identified a series of small-molecule fluoropyrimidine-based GLP-1R agonists. Optimization of the lead chemical series resulted in potent small-molecule agonists that activate the GLP-1R via a unique binding mode while signaling in a manner similar to that of peptide agonists. The series includes the clinical development candidate PF-06882961 (danuglipron), which we show has robust preclinical efficacy and oral bioavailability in healthy human participants.

RESULTS AND DISCUSSION

Development of a Sensitized Assay to Identify Weak GLP-1R Agonists. Binding of GLP-1 to its receptor activates the guanine (G) nucleotide-binding α stimulatory subunit (Gαs) of the heterotrimeric G protein complex, stimulating adenylate cyclase activity, and thereby increasing intracellular concentrations of cyclic adenosine monophosphate (cAMP).[19] Activation of the GLP-1R by GLP-1 also results in the recruitment of β-arrestin-1 (βArr1) and β-arrestin-2 (βArr2), which mediate receptor internalization and may serve as scaffolds for arrestin-dependent signaling.[20,21] The human GLP-1R shows no ligand-independent constitutive activity relative to other class B GPCRs (e.g., the gastric inhibitory polypeptide and parathyroid hormone 1 receptors),[22,23] which suggests a higher energy barrier for activation.[24] Multiple high-throughput screens had been conducted within Pfizer prior to this effort using binding or functional assays. The functional

https://doi.org/10.1021/acs.jmedchem.1c01856
J. Med. Chem. 2022, 65, 8208–8226

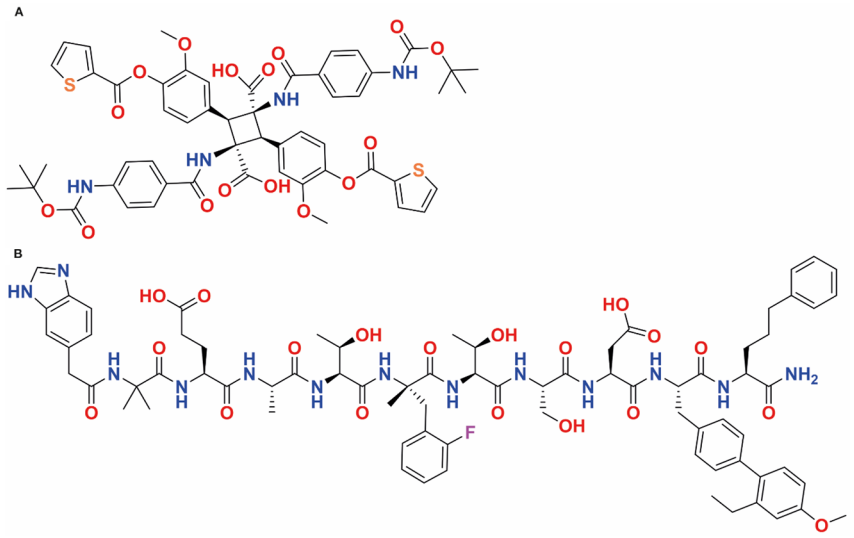

Figure 2. Structures of reference compounds. (A) Structure of Boc-5. (B) Structure of peptide **1**.

assays used cells with high levels of GLP-1R expression and/or amplified assay end points that had the potential to increase the sensitivity of the screen to detect weak agonists. Unfortunately, none of these efforts identified leads suitable for optimization to provide potent agonists. We hypothesized that a positive allosteric modulator (PAM) such as 4-[3-(benzyloxy)phenyl]-2-ethylsulfinyl-6-(trifluoromethyl)-pyrimidine (BETP) (Figure 1A) could be used to lower the activation energy barrier, thereby increasing assay sensitivity and facilitating the detection of weak agonists in a cell-based functional assay with moderate GLP-1R expression levels. The GLP-1R signaling of BETP has been characterized previously.[25−27] Using BETP, we observed potentiation of GLP-1R-mediated cAMP signaling in response to the weak nonpeptide GLP-1R agonist Boc-5[28] (Figure 2A) in Chinese hamster ovary (CHO) cells stably expressing the human GLP-1R (Figure 1B), as was also reported by Wootten et al.[29] In particular, we noted that the positive impact on the maximal effect (E_{max}) in this assay format would significantly improve the chances of identifying weak agonists during HTS at a single concentration. Further confidence in the assay design came from testing the effects of BETP on receptor-mediated β-arrestin (βArr) signaling. Peptide agonist **1** (Figure 2B), identified during our earlier efforts to design orally available peptidic GLP-1R agonists,[30] is a full (E_{max}) cAMP agonist (Figure 1C), but a partial βArr agonist (Figure 1D) at the GLP-1R. BETP improved the potencies of peptide **1** for both pathways and potentiated the E_{max} for βArr recruitment (Figure 1C,D and Table S1). The observed potentiation of the cAMP and βArr signaling pathways was consistent with our hypothesis that BETP treatment resulted in general receptor sensitization, rather than a pathway-specific signaling amplification.

Our BETP-sensitized cAMP screening assay (SA) (SA + BETP) was adapted to a single-point format and employed in an HTS of 2.8 million compounds from the Pfizer compound collection. A hit was defined by a threshold of a >30% effect (i.e., >30% of the E_{max} of GLP-1) at 10 μM, and the screen resulted in a low confirmed hit rate of 0.013%. A series of pyrimidine derivatives exemplified by **2** emerged from these hits (Figure 3A). Compound **2** was inactive as a GLP-1R agonist in the unpotentiated cAMP SA, which did not include BETP, but demonstrated an ∼70% effect at 20 μM in the presence of BETP (Figure 1E). This is considered a nontraditional screening approach as it carried the risk that the GLP-1R agonist lead series so identified might remain dependent on the presence of BETP to activate the receptor, and it was unclear at the outset whether we would observe GLP-1R agonism in the absence of BETP. However, it identified a hit series that would otherwise have been assessed as inactive and thus provided a starting point for medicinal chemistry optimization. As analogues were identified with improved cAMP potency in the BETP-sensitized assay, we also observed an increase in signaling efficacy in the absence of BETP (Figure 3B) to the point where a dose−response curve and the half-maximal effective concentration (EC_{50}) could be defined. For weaker agonists, BETP potentiated cAMP potency by ∼100-fold. As potency improved to <100 nM in the absence of BETP, the impact of the PAM gradually diminished (Figure 3C). The decreased level of potentiation of signaling by BETP as potency improved is consistent with the reported minimal effect of BETP on signaling of the potent GLP-1R endogenous agonist GLP-1, compared with the strong potentiation of the weaker agonist GLP-1(9−36)amide.[25]

Lead Series Optimization. In optimizing our lead series, we sought to improve the GLP-1R agonism by careful placement of polar groups with a minimal increase in molecular weight. In this ligand-driven optimization approach, we also explored conformational biases in the ligand that could potentially mimic the unknown receptor-bound conformation. Four structural regions were considered to improve GLP-1R agonist activity of the initial hit **2**: the piperidine ring, the benzyl ether, the 5-fluoro-pyrimidine, and the benzimidazole. The piperidine ring proved to be optimal in structure−activity relationship (SAR) studies, although other six-membered rings (e.g., piperazine, cyclohexane, etc.) also demonstrated GLP-1R agonism.[31,32] Likewise, the 4-chloro-2-fluoro-benzyl ether substituent was effective at activating the receptor. Small substituents at position 4 (e.g., chloro, fluoro, cyano, etc.) provided the greatest potency. Significant potency improvements were achieved by replacing the 5-fluoro-pyrimidine with a pyridyl group, presumably by biasing the preferred conformation of the pendent benzyl ether through repulsion of the oxygen and nitrogen lone pairs.[33] Removal of the fluorine likely favors the preferred torsion angle between the

https://doi.org/10.1021/acs.jmedchem.1c01856
J. Med. Chem. 2022, 65, 8208−8226

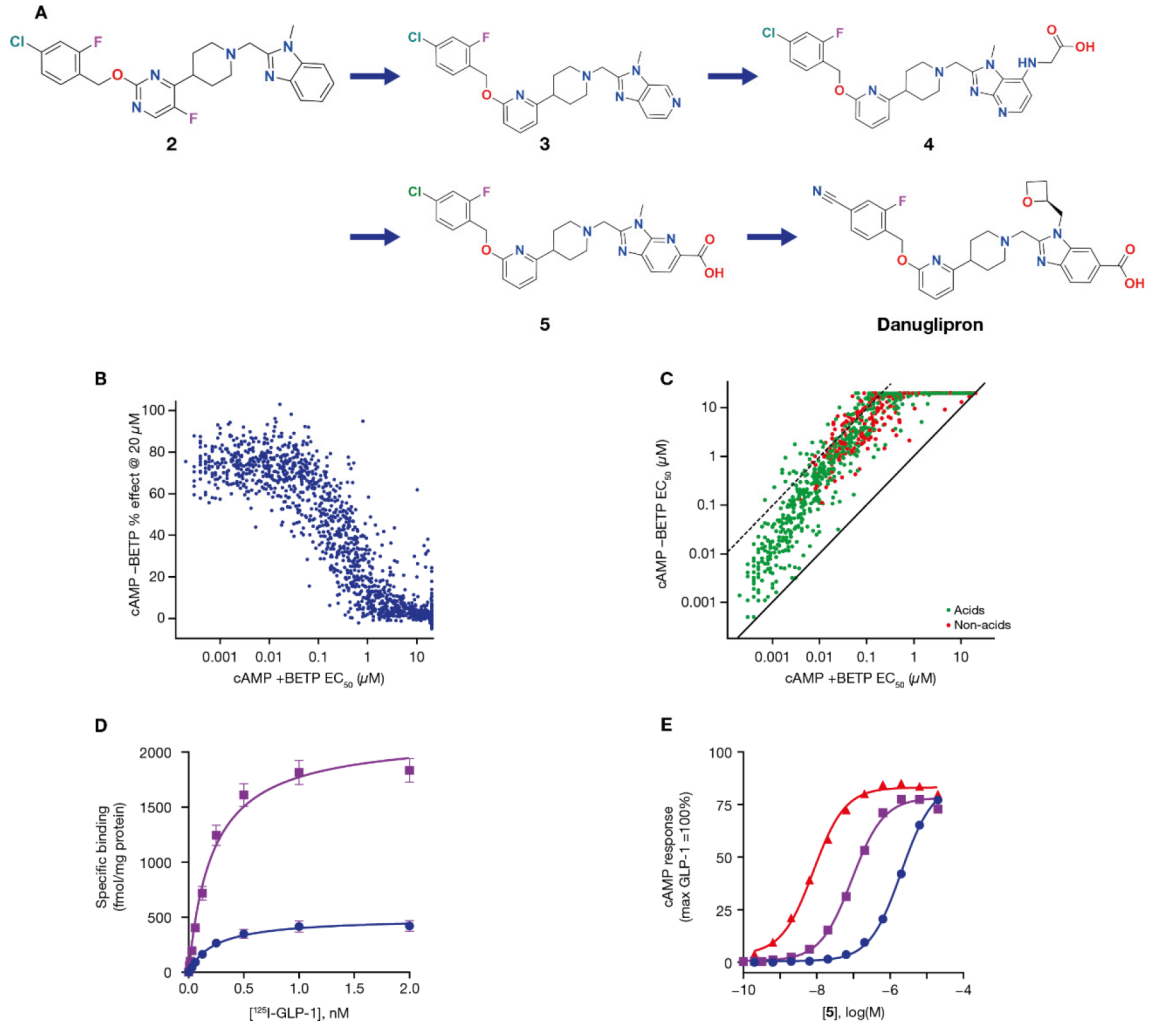

Figure 3. Optimization of small molecule **2** culminating in the identification of the clinical candidate danuglipron. (A) Structure of key compounds in the progression of small-molecule HTS hit **2** to clinical candidate danuglipron. Four structural regions were considered in our efforts to improve the GLP-1R agonist activity of **2**: the piperidine, the benzyl ether, the 5-fluoro-pyrimidine, and the benzimidazole. (B) Early evidence of activity in the cAMP assay without BETP. An increased level of cAMP acumulation (percent effect relative to 1 μM GLP-1) at a test compound concentration of 20 μM was observed in the absence of BETP as potency (EC_{50}) improved in the presence of BETP. Data from 1882 analogues. (C) Small-molecule agonist activity independent of BETP sensitization. Increased cAMP potency (EC_{50}) was observed in the absence of BETP as potency improved in the presence of BETP (red circles, non-acids; green circles, acid-containing analogues). Dashed line at a 100:1 EC_{50} ratio (−BETP/+BETP), solid line at a 1:1 ratio. Data from 1884 analogues. (D and E) Candidate selection CHO-GLP-1R cell line with a lower GLP-1R expression level confirms the efficacy-driven nature of small-molecule **5** agonism at the human GLP-1R. Data represent the mean ± SEM. (D) Saturation binding analysis in CHO cells expressing higher (purple squares, SA) and lower (blue circles, CS) human GLP-1R density. Data represent the mean ± SEM from two individual experiments performed in duplicate. (E) Small molecule **5** induced cAMP signaling in the CS cell line (blue circles), as well as in the SA in the presence (red triangles) or absence (purple squares) of BETP. Data represent the mean ± SEM from 81 (SA + BETP), 105 (SA + DMSO), or 87 (CS) independent experiments, each performed in duplicate; error bars are within the displayed symbols. cAMP data normalized using 100 nM (+BETP) or 1 μM (+DMSO) GLP-1 response (100%). Abbreviations: BETP, 4-[3-(benzyloxy)phenyl]-2-ethylsulfinyl-6-(trifluoromethyl)pyrimidine; cAMP, cyclic adenosine monophosphate; CHO, Chinese hamster ovary; CS, candidate selection; DMSO, dimethyl sulfoxide; EC_{50}, half-maximal effective concentration; GLP-1, glucagon-like peptide-1; GLP-1R, GLP-1 receptor; HTS, high-throughput screening; PAM, positive allosteric modulator; SA, screening assay; SEM, standard error of the mean.

aromatic and piperidine rings. Combining the pyridyl modification with a more polar 6-aza-benzimidazole led to **3** (EC_{50} = 77 nM in SA + BETP), which was >100-fold more potent than HTS hit **2** (Figure 3 and Table 1) and now active in the cAMP assay without BETP (SA EC_{50} = 2600 nM). It was also encouraging that this compound recruited βArr in the presence of BETP [EC_{50} = 9600 nM (Table 1)], suggesting the potential for minimal signaling bias. However, small molecule **3** was quite lipophilic (log $D_{7.4}$ = 5.7), resulting in high metabolic intrinsic clearance (CL_{int}) in human liver microsomes (HLM) [CL_{int} = 130 mL/min/kg (Table 2)]. The high lipophilicity was also associated with off-target pharmacology, such as inhibition of the human ether-a-go-go-related gene (hERG) ion channel [IC_{50} = 5.6 μM (Table 2)]. We sought further modifications to reduce lipophilicity and thereby reduce the metabolic clearance and improve the off-target profile.[34]

During our earlier efforts to identify orally available peptides,[30] we recognized the important role that carboxylic acid substituents played in activating the GLP-1R. Therefore, we sought to incorporate an acid substituent to improve both potency and physiochemical properties. In the absence of

https://doi.org/10.1021/acs.jmedchem.1c01856
J. Med. Chem. 2022, 65, 8208−8226

Table 1. Agonist-Mediated cAMP Accumulation in the BETP-Sensitized SA, Nonsensitized SA, and CS Cell Lines[a] and Agonist-Mediated βArr Recruitment with and without BETP in the DiscoverX Cell Line[b,c]

	SA cAMP + BETP[d]				SA cAMP − BETP[d]				CS cAMP[e]				βArr2 + BETP				βArr2 − BETP			
compound	EC_{50} (nM)	E_{max} (%)	slope	*N*	EC_{50} (nM)	E_{max} (%)	slope	*N*	EC_{50} (nM)	E_{max} (%)	slope	*N*	EC_{50} (nM)	E_{max} (%)	slope	*N*	EC_{50} (nM)	E_{max} (%)	slope	*N*
2	>9900 (5500–18000)	nd[f]	1.3 ± 0.75	8	>20000	na[g]	na[g]	7	>20000	na[g]	na[g]	2								
3	77 (62–95)	86 ± 12	0.89 ± 0.17	43	2600 (2100–3100)	79 ± 14	1.2 ± 0.26	47	>20000	na[g]	na[g]	4	9600 (6600–1400)	100 ± 3.8	0.97 ± 0.10	7	>30000	na[g]	na[g]	1
4	44 (23–85)	90 ± 15	0.76 ± 0.058	6	4600 (3300–6300)	100 ± 1.6	0.75 ± 0.18	6	>20000	na[g]	na[g]	3	1500 (1400, 1600)	23 (20, 27)	0.93 (0.98, 0.88)	2	>30000	na[g]		1
5	6.7 (5.6–7.9)	84 ± 10	0.97 ± 0.15	81	95 (84–110)	78 ± 9.5	1.1 ± 0.17	105	2100 (1900–2400)	87 ± 15	1 ± 0.14	87	2800 (740–11000)	99 ± 11	0.69 ± 0.13	3	>30000	na[g]		3
danuglipron	0.71 (0.35–1.4)	110 ± 6.0	0.98 ± 0.029	3	1.1 (0.61–1.9)	79 ± 6.2	1.1 ± 0.11	5	13 (9.9–17)	110 ± 13	1.1 ± 0.14	22								
PF-06883365	nt[h]				0.75 (0.34–1.7)	81 ± 7.3	0.98 ± 0.12	7	8.6 (4–19)	98 ± 11	1.1 ± 0.19	9								
exenatide	nt[h]				0.061 (0.035–0.11)	91 ± 14	1.1 ± 0.15	6	0.11 (0.075–0.17)	120 ± 15	1.4 ± 0.15	14								
liraglutide	nt[h]				0.39 (0.25–0.60)	94 ± 9.9	1.2 ± 0.16	6	0.95 (0.55–1.6)	120 ± 12	1.4 ± 0.14	12	nt[h]				17 (8.7–34)	120 ± 26	1.6 ± 0.22	6

[a]The EC_{50} value is expressed as the geometric mean with a 95% confidence interval (CI), while the E_{max} and slope values are reported as the arithmetic mean ± SD from the number of replicates indicated, each performed in duplicate. E_{max} data are presented relative to the response of 100 nM (+BETP) or 1 μM GLP-1 (100%). [b]The EC_{50} value is expressed as the geometric mean with 95% CI, while the E_{max} and slope values are reported as the arithmetic mean ± SD from the number of replicates indicated, each performed in duplicate. For $N = 2$, the two replicates are listed. E_{max} data are presented relative to the response of 1 μM GLP-1 (100%). [c]Conducted in assay medium. [d]cAMP production measured in the SA with or without BETP. [e]cAMP production measured in the CS cell line with or without BETP. [f]With a 60 ± 16% GLP-1 response at 20 μM. [g]Not applicable. [h]Not tested.

https://doi.org/10.1021/acs.jmedchem.1c01856
J. Med. Chem. 2022, 65, 8208−8226

Table 2. *In Vitro* Disposition and hERG Inhibition with Small-Molecule GLP-1R Agonists[a]

compound	log *D* (pH 7.4)	HLM CL_{int} (mL/min/kg)[d]	hHEP CL_{int} (μL/min/million)[d]	hERG[e] IC_{50} (μM)
2	5.6[b] ± 0.071 (n = 2)	>150 ± 120 (n = 3)	48 (n = 1)	5.4 (n = 1)
3	5.7[b] ± 0.28 (n = 2)	140 ± 46 (n = 3)	55 (n = 1)	5.6 (n = 1)
4	2.3[c] ± 0.028 (n = 2)	<11 ± 2.8 (n = 3)	37 ± 2.4 (n = 2)	>10 (n = 1)
5	2.0[c] ± 0.27 (n = 14)	29 ± 4.4 (n = 17)	31 ± 5.2 (n = 6)	>100 (n = 1)
danuglipron	1.8[c] ± 0.16 (n = 8)	<10 ± 1.9 (n = 7)	6.9 ± 1.8 (n = 12)	4.3 (3.3–4.7) (n = 7)

[a]The log *D*, HLM CL_{int}, and hHEP CL_{int} values are expressed as the arithmetic mean ± SD, while the hERG IC_{50} values are the geometric mean with a 95% CI, reported from the number of replicates indicated. [b]Log *D* was measured at pH 7.4 using the previously described RP-HPLC method.[36] [c]Shake-flash log *D* (SFlogD) was measured at pH 7.4 using the previously described shake-flash method.[37] [d]CL_{int} refers to total intrinsic metabolic clearance obtained from scaling *in vitro* half-lives of test compounds in HLM or cryopreserved hHEP as previously described.[38] [e]Inhibition of the hERG ion channel in a patch-clamp assay.

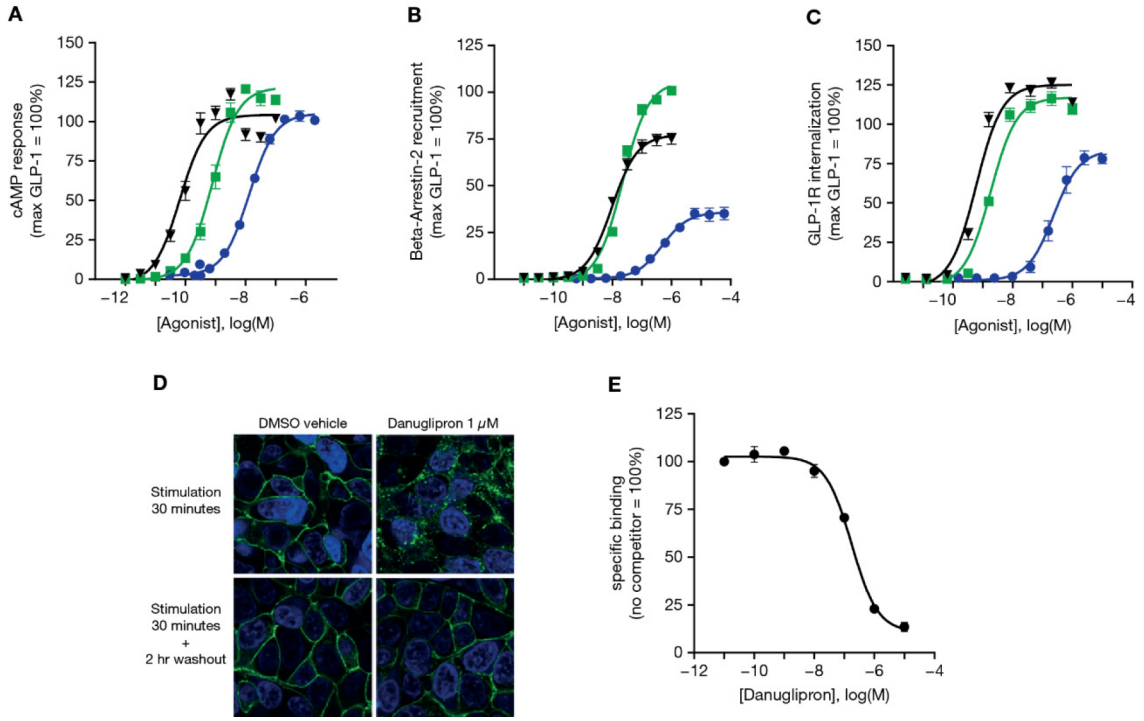

Figure 4. Molecular pharmacology of small-molecule GLP-1R agonist danuglipron. (A) cAMP concentration–response curves for exenatide (black inverted triangle), liraglutide (green squares), and danuglipron (blue circles) in the candidate selection cell line. Data represent the mean ± SEM from 14, 12, and 22 individual experiments, respectively, each performed in duplicate. (B) β-Arrestin recruitment concentration–response curves for exenatide (black inverted triangle), liraglutide (green squares), and danuglipron (blue circles). Data represent the mean ± SEM from four, four, and three individual experiments, respectively, each performed in duplicate. (C) GLP-1R agonist-driven receptor internalization assessed using the FAP-tagged human GLP-1R stably expressed in HEK 293 cells. Data represent the mean ± SEM from three independent experiments, each performed in triplicate. (D) Assessment of danuglipron-induced internalization and recycling of a GFP-tagged human GLP-1R (green) in a HEK 293 cell construct (blue nuclear staining) using confocal microscopy (representative images). (E) Competition binding curve for danuglipron using the [^{3}H]PF-06883365 probe. Data represent the mean ± SEM from four individual experiments, each performed in quadruplicate. cAMP, β-arrestin recruitment, and internalization data normalized to a 1 μM GLP-1 response (100%). In the curves, error bars are within the displayed symbols.

structural information for the GLP-1R, the design of acid-containing ligands was driven by SAR and the observation that polarity was better tolerated in the benzimidazole region. Introduction of a carboxylic acid-containing substituent at position 7 of the benzimidazole yielded **4** (Figure 3 and Table 1). Compound **4** demonstrated potency comparable to that of **3** [EC_{50} = 4.6 μM (Table 1)], but with a markedly lower lipophilicity (log $D_{7.4}$ = 2.3) (Table 2), indicating that the acid was likely making a productive interaction.[35] A carboxylic acid directly attached to position 6 of the benzimidazole proved to be optimal for potency. For example, **5** (Figure 3A) was a potent GLP-1R agonist [SA EC_{50} = 95 nM (Table 1)] with improved ability to recruit βArr in the presence of BETP [EC_{50} = 2800 nM (Table 1)] relative to **3**. Compound **5** exhibited a moderate CL_{int} in HLM (29 mL/min/kg) and human hepatocyte [31 μL min^{-1} (million cells)$^{-1}$] metabolic stability assays and excellent selectivity against the hERG channel [>100 μM (Table 2)].

We then sought a less sensitive functional assay with reduced receptor expression levels to enable the optimization of efficacy-driven GLP-1R agonists for clinical development. Less sensitive cell assays are valuable for distinguishing the contributions of affinity and efficacy in the cellular response to an agonist.[39] Considering the lack of robust cellular models for the endogenous human GLP-1R, we developed a cell line with a GLP-1R density comparable with endogenous tissue levels.[40]

https://doi.org/10.1021/acs.jmedchem.1c01856
J. Med. Chem. 2022, 65, 8208–8226

Table 3. Agonist-Mediated βArr Recruitment and Receptor Internalization and Recruitment of βArr1 and βArr2 by Agonists in the DiscoverX Cell Line and Internalization of the FAP-Tagged GLP-1R in HEK 293 Cells[a]

	βArr1[b]				βArr2[b]				internalization		
compound	EC_{50} (nM)	E_{max} (%)	slope	N	EC_{50} (nM)	E_{max} (%)	slope	N	EC_{50} (nM)	E_{max} (%)	N
danuglipron	760 (530−1100)	41 ± 0.98	0.90 ± 0.067	3	490 (310−760)	36 ± 9.8	1 ± 0.18	3	230 (160−350)	83 ± 3.2	3
PF-06883365	250 (200−330)	50 ± 11	0.94 ± 0.013	3	610 (180−2100)	50 ± 9.8	0.79 ± 0.12	6	not tested		
exenatide	14 (9.2−23)	70 ± 9.5	1.2 ± 0.079	4	9 (7.4−11)	75 ± 7.6	1.3 ± 0.13	4	0.60 (0.42−0.84)	125 ± 2.8	3
liraglutide	34 (19−63)	96 ± 5.3	1.4 ± 0.26	4	20 (15−26)	99 ± 1.4	1.6 ± 0.11	4	1.8 (1.4−2.5)	117 ± 2.6	3

[a]Conducted in a buffer containing 0.1% BSA. [b]The EC_{50} value is expressed as the geometric mean with a 95% CI, while the E_{max} and slope values are reported as the arithmetic mean ± SD from the number of replicates indicated, each performed in duplicate. When $N = 2$, the two replicates are listed. E_{max} data are presented relative to the response of 1 μM GLP-1 (100%) for βArr assays and relative to the maximal effect of GLP-1 (100%) for receptor internalization.

Table 4. Competition Binding Affinities

	[^{125}I]GLP-1 binding			[^{3}H]PF-06883365 binding		
compound	K_i (nM)[a]	slope	N	K_i (nM)[a]	slope	N
danuglipron	360 (140−920)	0.70 ± 0.099	4	80 (62−91)	1[b]	4
PF-06883365	not tested		−	51 (43−61)	1.0 ± 0.15	16
exenatide	0.092 (0.073−0.12)	0.94 ± 0.11	17	0.053	not available	1
liraglutide	4.4 (3.4−5.5)	0.83 ± 0.17	19	6.3	not available	1

[a]The K_i value is expressed as the geometric mean with a 95% CI performed in duplicate, while the slopes are reported as the arithmetic mean ± SD from the number of replicates indicated, each performed in duplicate. When $N = 1$, the replicates are listed. [b]Analyzed using a three-parameter model.

The receptor density (Figure 3D) for this candidate selection (CS) cell line (CS B_{max} = 500 ± 28 fmol/mg) was ∼4.3-fold lower than that of the cell line used for primary screens (SA B_{max} = 2200 ± 80 fmol/mg). In the setting of lower GLP-1R levels in this CS cell line, small molecule **5** remained a full agonist (Figure 3E) but was ∼20-fold less potent [CS EC_{50} = 2.1 μM (Table 1)], suggesting that further potency improvements would be required. Optimizing the substituent on the benzimidazole nitrogen proved to be a fruitful approach for improving potency without detrimentally impacting physiochemical properties, with smaller, more polar groups preferred. For example, a methylene-linked oxetane increased potency ∼100-fold relative to that of the methyl substituent in **5**, leading to the identification of PF-06882961 (danuglipron), which was a full agonist (EC_{50} = 13 nM) in the CS cAMP assay (Figure 4A and Table 1). Danuglipron also incorporates a nitrile replacement for the chloride in the benzyl ether region, which served to reduce CL_{int} in HLM (<10 mL/min/kg) as well as in human hepatocytes (6.9 μL/min/million cells) (Table 2).

Molecular Pharmacology of Danuglipron. In developing a small-molecule GLP-1R agonist, we sought *in vitro* signaling profiles that were comparable to those of marketed GLP-IR peptide agonists, as the individual contributions of cAMP signaling and βArr recruitment pathways toward the therapeutic efficacy of marketed GLP-1R agonists remain ill-defined.[20,21] As such, danuglipron agonist activity at both the cAMP and βArr pathways was assessed and compared to that of the marketed GLP-1R agonists exenatide and liraglutide. The potency of danuglipron (CS EC_{50} = 13 nM) on the cAMP pathway was approximately 120- and 14-fold (Figure 4A and Table 1) lower than those of exenatide (CS EC_{50} = 0.11 nM) and liraglutide (CS EC_{50} = 0.95 nM), respectively. The ability of danuglipron and marketed peptides to engage βArr was further assessed using PathHunter technology (Figure 4B and Table 3). Danuglipron was a partial agonist in recruiting βArr2 (EC_{50} = 490 nM; E_{max} = 36%), while exenatide (βArr2 EC_{50} = 9.0 nM; E_{max} = 75%) and liraglutide (βArr2 EC_{50} = 20 nM; E_{max} = 99%) were 54- and 23-fold more potent, respectively, with greater E_{max} values. The responses of βArr1 closely mirrored those of βArr2 (Table 3). Calculation of pathway bias[41] supports the idea that relative to liraglutide, both danuglipron and exenatide display statistically significant signaling bias toward the cAMP pathway relative to βArr1 and βArr2 recruitment (Table S2). These data are consistent with a recent publication reporting that relative to GLP-1, danuglipron exhibits subtle bias for cAMP, relative to βArr1 recruitment.[42]

βArr recruitment at the GLP-1R leads to internalization of the receptor toward endosomal compartments, which has been proposed to impact receptor desensitization and signaling duration in preclinical models.[20,21] As a complementary approach to probing GLP-1R function, we quantified agonist-induced GLP-1R internalization using human embryonic kidney (HEK) 293 cells stably expressing a fluorogen-activated protein (FAP)-tagged version of the human GLP-1R (Figure 4C). Initial experiments confirmed that danuglipron and peptide agonists retain similar rank order potency and full cAMP signaling in this HEK 293 model relative to the CS assay (Figure S1). In follow-up experiments using this cell model, treatment with danuglipron led to FAP-GLP-1R internalization (EC_{50} = 230 nM; E_{max} = 83%). Exenatide (EC_{50} = 0.60 nM; E_{max} = 125%) and liraglutide (EC_{50} = 1.8 nM; E_{max} = 117%) were 380- and 130-fold more potent, respectively, and caused somewhat greater receptor internalization relative to danuglipron (Table 3). Pathway bias analysis using parameters derived from this cellular model further supports that, relative to liraglutide, danuglipron has a minor (3.6-fold), statistically significant bias away from internalization (relative to cAMP) (Table S2). Finally, agonist-induced internalization and recycling of a green fluorescent protein (GFP)-tagged human GLP-1R construct expressed in HEK 293 cells were visualized using confocal microscopy (Figure 4D). Consistent with the FAP-based approach, stimulation

https://doi.org/10.1021/acs.jmedchem.1c01856
J. Med. Chem. 2022, 65, 8208−8226

with danuglipron for 30 min triggered marked intracellular accumulation of the GFP-GLP-1R, which was reversible following a 2 h washout period.

To further define the pharmacological profile of danuglipron, we sought to determine its binding affinity using radioligand binding assays. In competition experiments using [^{125}I]GLP-1 as the radiolabeled probe, the inhibition constant (K_i) of danuglipron for the GLP-1R (K_i = 360 nM) (Figure 4E) was 3900- and 82-fold higher than those of exenatide (K_i = 0.092 nM) and liraglutide (K_i = 4.4 nM), respectively (Table 4). However, given that large peptides like GLP-1 interact with the extracellular and transmembrane domains of the GLP-1R,[43] and that our small molecules were unlikely to recapitulate this complex binding mode, it was unclear whether such competition binding experiments with radiolabeled GLP-1 were providing an accurate measure of affinity.[30] Therefore, we also developed a novel radiolabeled small-molecule probe, [^{3}H]PF-06883365, which is expected to bind in the same pocket as danuglipron (Figure 5A,B and Table 4). The affinity of danuglipron (K_i = 80 nM) measured using this new radioligand was 4.5-fold more potent and more consistent with its cAMP potency, whereas the marketed peptides had similar affinities using both radioligands (Table 4). The observed binding affinities of danuglipron in these assays translated to plasma levels that were expected to be readily achieved with a small molecule following oral administration.

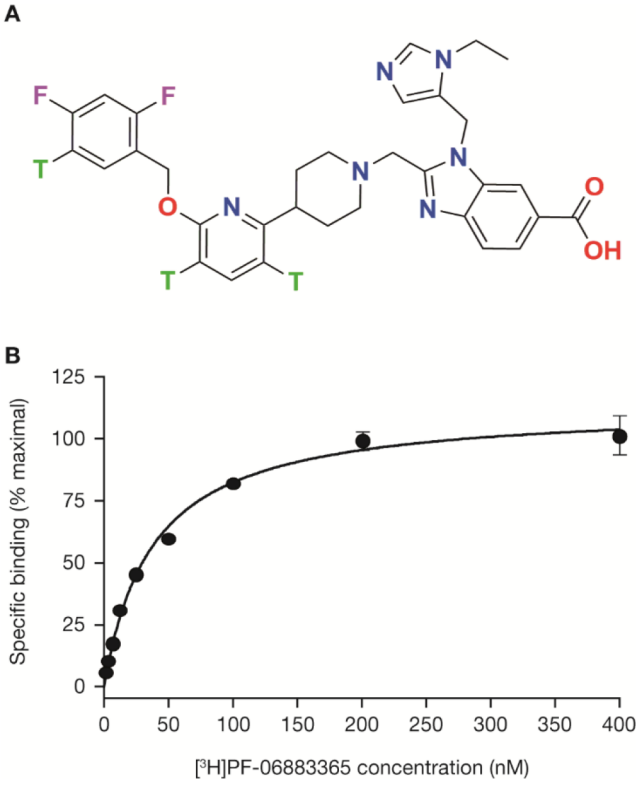

Figure 5. Binding affinity of danuglipron, as evaluated using a competition binding assay based on radiolabeled small-molecule agonist [^{3}H]PF-06883365. (A) Structure of the small-molecule agonist radioligand [^{3}H]PF-06883365. (B) Saturation binding analysis for [^{3}H]PF-06883365 showed that [^{3}H]PF-06883365 binds plasma membranes from CHO cells stably expressing a high density of the hGLP-1R ("binding cell line") with an averaged K_d of 38 nM and a B_{max} of 5470 fmol/mg. Data represent the mean ± SEM from two independent experiments, each performed in quadruplicate; error bars are within the displayed symbols.

Tryptophan 33 in the GLP-1R Is Required for Danuglipron Signaling. Prior to the selection of animal models for *in vivo* pharmacology studies, we characterized the potential for species differences in GLP-1R activation with our small-molecule agonists. Danuglipron stimulated cAMP accumulation in CHO cells expressing both the human and monkey GLP-1Rs with comparable EC_{50} values (Figure 6A,B).

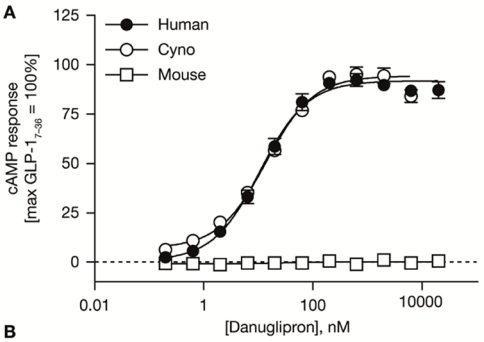

B

Species	EC_{50} (nM), free (95% CI)	E_{max} (%) (95% CI)	*n*
Cynomolgus macaque	4.4 (2.3–7.5)	95 (80.6–109.3)	5
Rat	>20,000	N.M.	3
Rabbit	>20,000	N.M.	3
Mouse	>20,000	N.M.	3

Figure 6. Functional activity of danuglipron at the GLP-1R stably expressed by CHO cells, as assessed using cAMP accumulation assays. (A) cAMP accumulation in CHO cells expressing either the human, cynomolgus monkey, or mouse GLP-1. Data represent the mean ± SEM. (B) EC_{50} values of danuglipron at the cynomolgus monkey, rat, rabbit, and mouse GLP-1R stably expressed in CHO cells. The EC_{50} value is expressed as the geometric mean with a 95% confidence interval, while the E_{max} value is reported as the arithmetic mean with the standard deviation for the number of replicates indicated; error bars are within the displayed symbols. Data normalized to the 1 μM GLP-1 response (100%).

In contrast, danuglipron did not increase cAMP levels in cells expressing the mouse, rat, or rabbit GLP-1R. Consistent with this finding, no improvement in glucose tolerance was observed during an intraperitoneal glucose tolerance test in C57BL6 mice that were administered a subcutaneous dose of danuglipron (10 mg/kg) (Figure 7A).

Comparison of the GLP-1R sequences in human and monkey versus other species revealed the notable presence of a tryptophan (W) residue at position 33 of the primate GLP-1R. In contrast, other species, including the mouse, rat, and rabbit GLP-1R, contain a serine (S) residue at position 33. Supporting the crucial role of W33, danuglipron increased the level of accumulation of cAMP in cells expressing the S33W mutant of mouse GLP-1R, whereas it failed to induce signaling at the human W33S receptor (Figure 7B). In contrast, cAMP signaling in response to GLP-1 was comparable between wild-type and mutant receptors, supporting the hypothesis that altered signaling with danuglipron was not due to a marked alteration of surface expression for the mutated constructs (Figure 7C). These observations are interesting considering that W33 is located on the extracellular domain (ECD), distal from the transmembrane domains and connecting loops directly involved in peptide-induced GPCR

https://doi.org/10.1021/acs.jmedchem.1c01856
J. Med. Chem. 2022, 65, 8208−8226

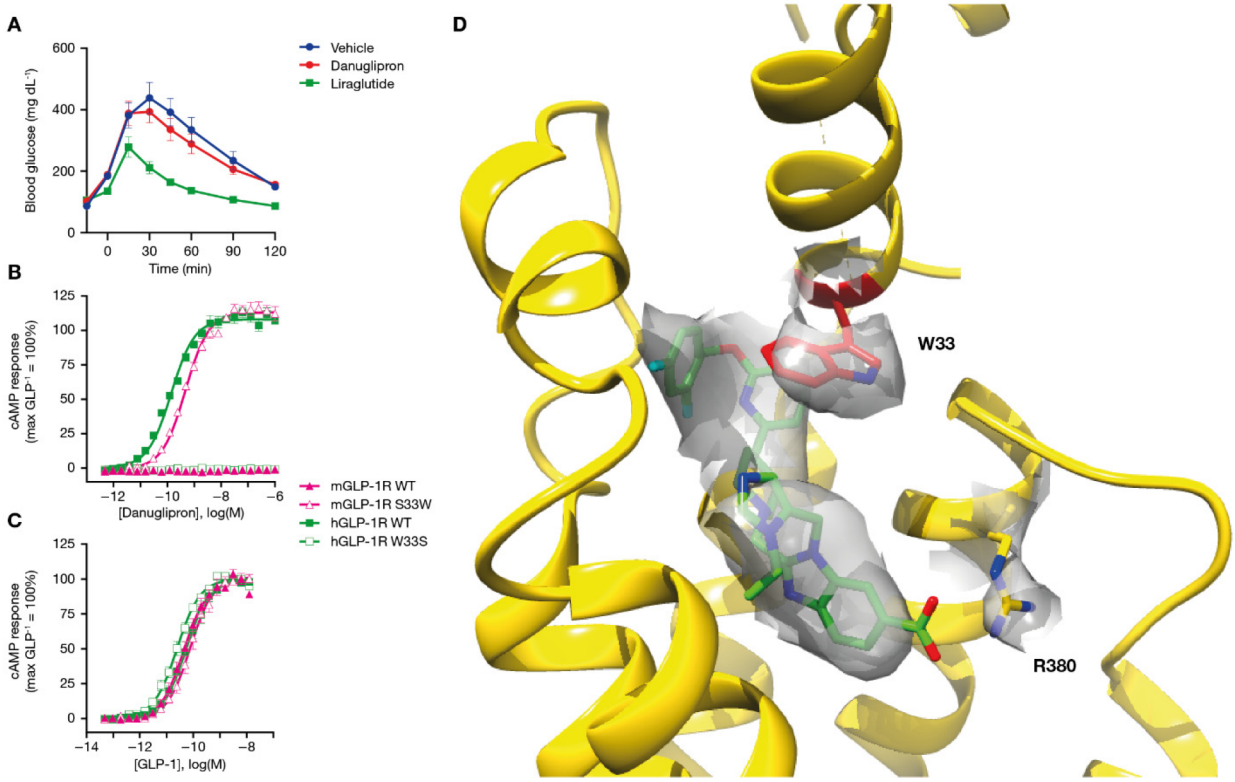

Figure 7. Tryptophan 33 is critical for the function of small-molecule GLP-1R agonists. (A) In contrast to liraglutide, danuglipron does not reduce glucose AUC during an intraperitoneal glucose tolerance test in C57BL/6 mice. (B and C) In contrast to GLP-1, danuglipron promotes cAMP production in GLP-1R-expressing cells only when residue 33 is tryptophan (W), not serine (S). (B) Danuglipron signals in CHO cells expressing human GLP-1R (filled green squares), but not the mouse GLP-1R (filled pink triangles). Danuglipron signaling is restored in CHO cells expressing mouse GLP-1R S33W (empty pink triangles) and is negated in human GLP-1R W33S (empty green squares). (C) GLP-1 promotes signaling in mouse and human wild-type and mutant constructs. (D) Cryogenic electron microscope (cryo-EM) structure of PF-06883365 (green) bound to the human GLP-1R illustrating the map density around the ligand (Protein Data Bank entry 7S15). W33 closes the top of the small-molecule binding pocket. Arginine 380 (R380) interacts with the carboxylic substituent of the small-molecule agonist. Helix 4 was omitted for the sake of clarity (panel D prepared with Chimera).[44] Data represent the mean ± SEM, and error bars are within the displayed symbols. cAMP data are from three independent experiments, each performed in duplicate, and normalized to the 1 μM GLP-1 response (100%).

Table 5. Preclinical Pharmacokinetic Parameters of Danuglipron

species[a]	dose (mg/kg)	C_{max} (ng/mL)	T_{max} (h)	$AUC_{0-\infty}$ (ng h mL^{-1})	CL_p (mL/min/kg)	Vd_{ss} (L/kg)	$t_{1/2}$ (h)	oral F (%)[b]
rat	1.0 (iv)	–	–	296 ± 39.8	57.3 ± 8.68	0.86 ± 0.38	1.13 ± 0.84	–
	5.0 (po)[b]	141 (153, 128)	0.5 (0.5, 0.5)	168 (151, 184)	–	–	0.63 (0.46, 0.79)	11 (10, 12)
	100 (po)[b]	2820 (2580, 3060)	0.75 (0.5, 1.0)	11900 (10300, 13500)	–	–	2.37 (2.25, 2.49)	39 (37, 44)
monkey	1.0 (iv)	–	–	1240 (1390, 1080)	13.8 (12.0, 15.5)	0.266 (0.268, 0.264)	1.89 (2.03, 1.74)	–
	5.0 (po)[b]	68.7 (86.3, 51.0)	1.5 (2.0, 1.0)	303 (363, 242)	–	–	6.92 (5.71, 8.11)	5.0 (4.0, 6.0)
	100 (po)[b]	1150 ± 715	3.3 ± 2.5	11000 ± 3500	–	–	6.37	9.0

[a]All experiments involving animals were conducted in our AAALAC-accredited facilities and were reviewed and approved by Pfizer Institutional Animal Care and Use Committee. Pharmacokinetic parameters were calculated from plasma concentration−time data and are reported as mean ± SD for n = 3−4 and maximum values for n = 2. All pharmacokinetic studies were conducted in males of each species (Wistar rats and cynomolgus monkey). The iv doses for danuglipron were administered as a solution in a 5:95 (v/v) polyethylene glycol 400/12% (w/v) sulfobutyl-β-cyclodextrin in water mixture or in a 10:50:40 (v/v/v) DMSO/polyethylene glycol 400/deionized water mixture. Oral pharmacokinetic studies were conducted in the fasted state using the crystalline-free form of the 2-amino-2-hydroxymethylpropane-1,3-diol (Tris) salt form of danuglipron. For oral pharmacokinetic studies, danuglipron, Tris salt was formulated in a 2:98 (v/v) Tween 80/0.5% (w/v) methyl cellulose A4M in distilled water mixture. [b]Danuglipron, Tris salt.

activation.[22,43] Overall, our findings were reminiscent of a previous report describing the 100-fold reduction in the binding affinity of the small-molecule GLP-1R antagonist T-0632 in the W33S mutant of the human GLP-1R.[45] It was postulated that the binding of T-0632 stabilizes a closed, inactive conformation of the GLP-1R, which involves W33.[46]

Recent cryo-EM structures of the human and rabbit GLP-1Rs bound to GLP-1 indicate that residue 33 does not interact with peptide agonists but extends toward solvent (Figure S2).[43,47] Moreover, the species selectivity of a GLP-1R monoclonal antibody (Fab 3F52) was attributed to a binding epitope containing W33,[48,49] which further supports the

https://doi.org/10.1021/acs.jmedchem.1c01856
J. Med. Chem. 2022, 65, 8208−8226

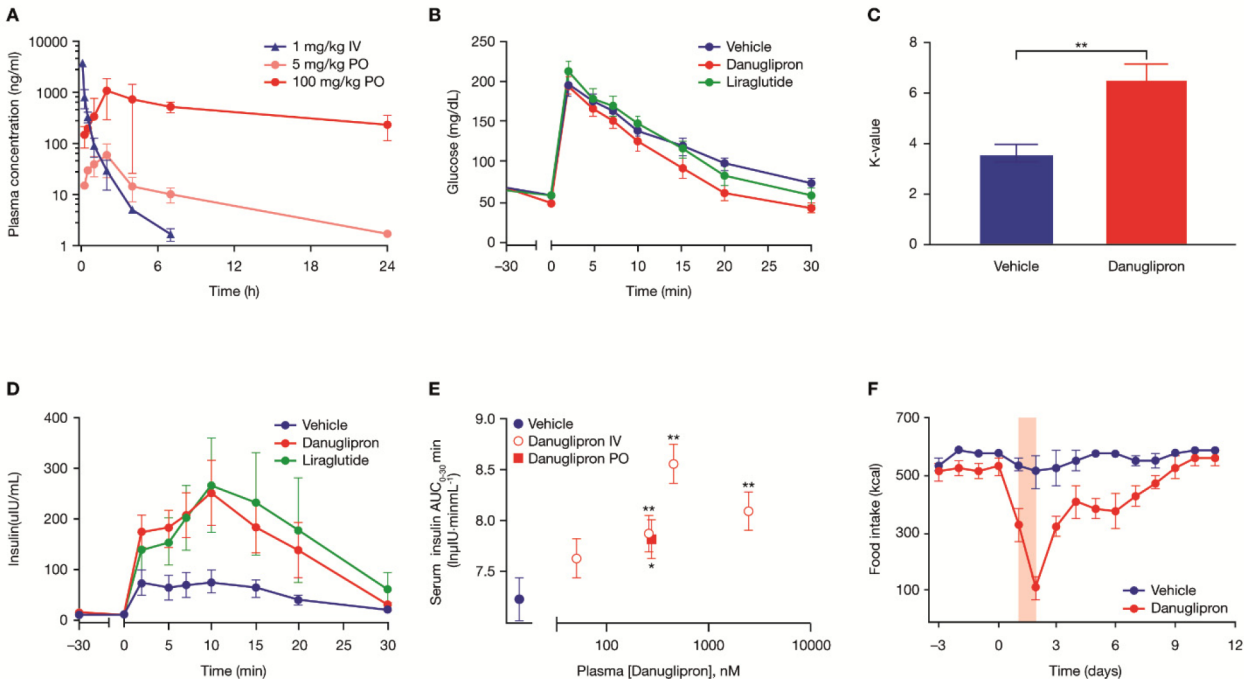

Figure 8. Danuglipron potentiates glucose-stimulated insulin release and reduces the rate of food intake in monkeys. (A) Profile of danuglipron plasma concentration vs time after intravenous (iv) or oral (po) dosing in male cynomolgus monkeys (n = 2 each). (B–E) Danuglipron increased the rate of glucose disappearance and enhanced insulin secretion during an iv glucose tolerance test (IVGTT) (250 mg of 50% dextrose/kg) in cynomolgus monkeys (n = 8 each). (B) Serum glucose, (C) K value, and (D) serum insulin during the IVGTT when danuglipron was iv infused to 3.0 μM (55 nM unbound) serum levels; liraglutide was administered by subcutaneous injection to achieve 58 nM (0.31 nM unbound) serum levels. (E) iv and po (100 mg/kg) administration of danuglipron potentiated glucose-stimulated insulin release ($AUC_{0-30\ min}$) in an exposure-proportional manner during an IVGTT. (F) Food intake in monkeys treated with either vehicle or subcutaneously administered danuglipron (2.9 mg/kg) once daily for 2 days (n = 6 each) (orange band). All values are presented as mean ± SEM. *p < 0.05 and **p < 0.01 vs vehicle (mixed model comparisons between LS-Means estimates).

hypothesis that W33 is solvent-exposed. To better understand the role of W33 in the binding of a small-molecule agonist to the GLP-1R, we generated a cryo-EM structure of a danuglipron analogue (PF-06883365) bound to the human GLP-1R (Figure 7D). To overcome the low yield and instability of the GLP-1R, eight individual thermostabilizing mutations (I146Y, A208R, Q213E, S219R, F260A, Y291A, L339E, and K346Q) were identified and introduced into the WT GLP-1R to generate the final thermostabilized receptor (GLP1-R StaR 8.2), which facilitated structural studies without a significant impact on receptor pharmacology as depicted in Table S3. In this structure, the GLP-1R ECD has rotated slightly relative to the peptide-bound structures, and W33 has moved ∼14 Å, closing the top of the small-molecule binding pocket. Consistent with the potency gains achieved via introduction of the carboxylic acid group at position C6 on the benzimidazole ring, the cryo-EM structure suggested that the carboxylic acid motif in PF-06883365 forms a productive ion-pair interaction with an arginine residue at position 380 in the GLP-1R-binding pocket. This interaction is clearly observed in the cryo-EM structure of danuglipron bound to GLP-1R,[42] which was determined at the higher resolution of 2.5 Å. During the preparation of this work, several other GLP-1R small-molecule agonist-bound structures that do not engage R380 have been published, for example, CHU-128,[42] LY3502970z,[50] and TT-OAD240[51] that bind to the GLP-1R in a manner significantly different from the observed binding of our small molecules.

Danuglipron Is Orally Bioavailable and Efficacious in Decreasing the Level of Glucose and Food Intake in Monkeys. The pharmacokinetics of danuglipron were examined in male Wistar rats and male cynomolgus monkeys after intravenous (iv) and oral (po) administration (Figure 6A and Table 5).

Following iv administration, danuglipron demonstrated moderate to high plasma clearance (CL_p) values in rats (CL_p = 57.3 mL/min/kg) and monkeys [CL_p = 13.8 mL/min/kg (Figure 8a)] with relatively short elimination half-lives of 1.1 and 1.9 h in rats and monkeys, respectively. The oral bioavailability of a Tris salt form of danuglipron in animals was low to moderate and increased in a dose-dependent manner, which was adequate for studying the preclinical *in vivo* efficacy and safety of danuglipron delivered via oral gavage in a standard 0.5% methyl cellulose formulation containing 2% Tween 80.

Because danuglipron does not activate the rodent GLP-1R, the therapeutic effects of danuglipron on insulin and glucose were examined in an intravenous glucose tolerance test (IVGTT) in cynomolgus monkeys following iv infusion and po administration. Infusion rates and po doses were projected using systemic concentrations from monkey pharmacokinetic (PK) studies that were required to achieve receptor occupancies (RO) bracketing the RO estimated from the reported human plasma exposures for liraglutide at its clinically efficacious dose (1.8 mg once daily). The iv infusion of danuglipron during the IVGTT led to an increase in the rate of insulin secretion and the rate of glucose disappearance (K

https://doi.org/10.1021/acs.jmedchem.1c01856
J. Med. Chem. 2022, 65, 8208−8226

value) (Figure 8B−D). Enhancement of glucose-stimulated insulin secretion by danuglipron was concentration-dependent and comparable following the po dosing and iv infusion routes (Figure 8E). Once-daily subcutaneous administration of danuglipron for 2 days also inhibited food intake compared with that of vehicle-treated monkeys (Figure 8F). The subcutaneous route of administration was chosen to reduce variability in systemic exposure noted upon po administration and was more convenient than iv administration.

Oral Administration of Danuglipron Was Well Tolerated with Dose-Proportional Systemic Exposure Increases in Healthy Human Study Participants. Danuglipron was selected as a candidate for clinical studies on the basis of its *in vitro* and *in vivo* pharmacological and disposition profile, including potent agonism of the GLP-1R, preclinical disposition attributes (e.g., low metabolic CL_{int} in human hepatocytes), good safety margins versus the hERG channel [IC_{50} = 4.3 μM (Table 2)], and broad panel screening (Table S4), and selectivity versus related class B GPCRs (Table S5). Moreover, adequate safety margins were observed in repeat dose rat and monkey toxicology studies, which supported advancing danuglipron to human clinical studies.

The safety, tolerability, and pharmacokinetics of danuglipron were evaluated in a first-in-human, Phase 1, randomized, double-blind, placebo-controlled, single ascending dose study in healthy adult participants. A total of 25 participants in three cohorts were randomized to receive study treatment. Data from the dose-escalation portion of the study (cohorts 1 and 2) are presented herein; in this portion of the study, 17 participants received immediate release tablet formulations of danuglipron or a matching placebo at single doses ranging from 3 to 300 mg. Following po administration under fasted conditions, danuglipron was generally well tolerated. There were no serious or severe adverse events (AEs) reported, nor discontinuations due to AEs (Table S6). Most AEs were mild in severity, and a higher proportion of participants reported an AE following administration of danuglipron at the 300 mg dose level compared with other study treatments (Table S6). The most common AEs recorded following administration of danuglipron were nausea, vomiting, and decreased appetite, all of which were considered treatment-related and consistent with the expected effects of the GLP-1R agonist mechanism. Plasma exposure of danuglipron, as measured by maximal plasma concentrations (C_{max}) and area under the curve from time 0 extrapolated to infinity (AUC_{inf}), increased in an approximately dose-proportional manner, with the mean $t_{1/2}$ ranging from 4.3 to 6.1 h (Figure 9 and Table S7).

The median time (T_{max}) to C_{max} values ranged from 2.0 to 6.0 h post-dose. An immediate release tablet formulation of danuglipron was also administered under fed conditions at a dose of 100 mg. The pharmacokinetics (AUC_{inf} and $t_{1/2}$) of danuglipron were similar under fed or fasting conditions (Table S7), indicating that danuglipron can be dosed in both the fed and fasted states, a major advancement in the field. As such, it could be expected that patient adherence to danuglipron will be robust[12] and, consequently, that safety and efficacy profiles will be stable.

The primary and secondary end points of the study were safety and pharmacokinetic parameters, and fasting serum glucose was measured pre-dose and post-dose in study participants, all of whom had glucose and glycated hemoglobin (HbA1c) levels within the normal reference range for the laboratory. After the administration of single doses of

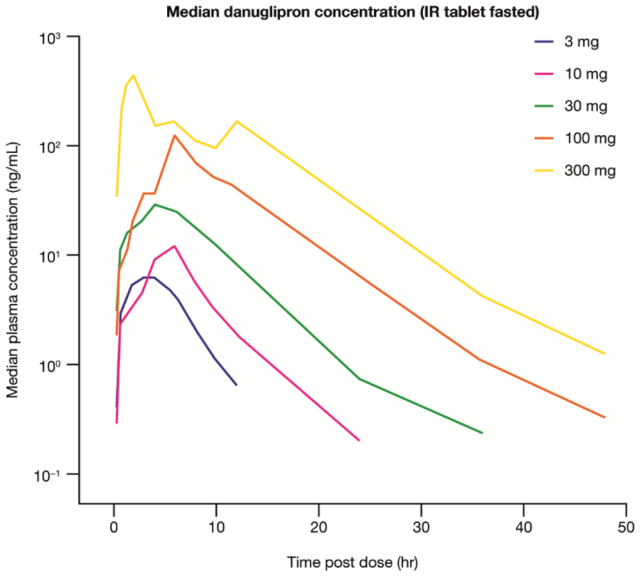

Figure 9. Median plasma danuglipron concentration−time profiles after single-dose oral administration of danuglipron (3−300 mg) to humans (n = 6/dose, except n = 12 in the 300 mg group) in the fasted state. Plasma exposure increased in an approximately dose-proportional manner, as assessed by dose-normalized geometric mean C_{max} and AUC_{inf}, with a mean $t_{1/2}$ ranging from 4.3 to 6.1 h. The median time to C_{max} (T_{max}) values ranged from 2.0 to 6.0 h post-dose. The human pharmacokinetic parameters of danuglipron with associated statistics are listed in Table S7. IR, immediate release.

danuglipron, all post-dose glucose levels remained within the normal reference range for the laboratory. As these were healthy patients and large changes in glucose were not expected, no AEs of hypoglycemia were reported.

A Phase 1 study with danuglipron has been recently completed, showing favorable efficacy and safety of multiple doses of danuglipron over 4 weeks of treatment in participants with T2DM.[52] Longer Phase 2 studies of danuglipron will need to be conducted in subjects with T2DM to determine optimal dosing for sustained glycemic control.

Synthesis of Danuglipron. The multigram synthesis of danuglipron to support PK and *in vivo* studies is described in Schemes 1−3. The synthesis of N-Boc piperidine **9** began from commercially available 2,6-dichloropyridine (**6**) and ester **7**. Deprotonation of **7** with LiHMDS to its lithium enolate followed by S_NAr with **6** provided **8** in 45% yield. Saponification and subsequent decarboxylation of **8** gave N-Boc piperidine **9**, which was subjected to Buchwald−Hartwig etherification and deprotection to furnish piperidine **12** as the bis-tosylate salt (Scheme 1).

The synthesis of benzimidazole **18** started with a S_NAr reaction between (*S*)-oxetan-2-ylmethanamine (**13**) and methyl-3-fluoro-4-nitrobenzoate (**14**) in MeCN to afford nitro ester **15**.[a] Reduction of the nitro group by catalytic hydrogenation over Pd/C provided dianiline **16**. Treatment of **16** with orthoester **17** in MeCN with catalytic pTSA provided an 83% yield of chloromethyl benzimidazole **18**.

The union of the two main fragments, piperidine **12** with benzimidazole **18**, under basic conditions provided the penultimate ester intermediate **19**. After extensive evaluation of the conditions, saponification of **19** was affected by treatment with 2 equiv of 1,5,7-triazabicyclo[4.4.0]dec-5-ene (TBD) in a water/MeCN mixture. This judicious choice of

https://doi.org/10.1021/acs.jmedchem.1c01856
J. Med. Chem. 2022, 65, 8208−8226

Scheme 1. Synthesis of Piperidine 12

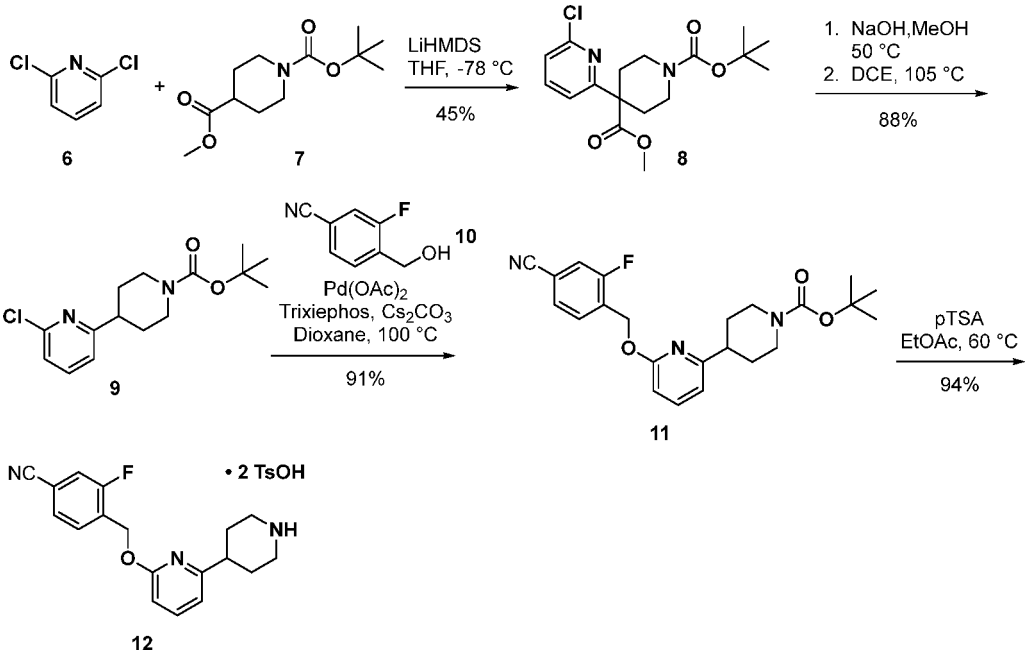

Scheme 2. Synthesis of Benzimidazole 18

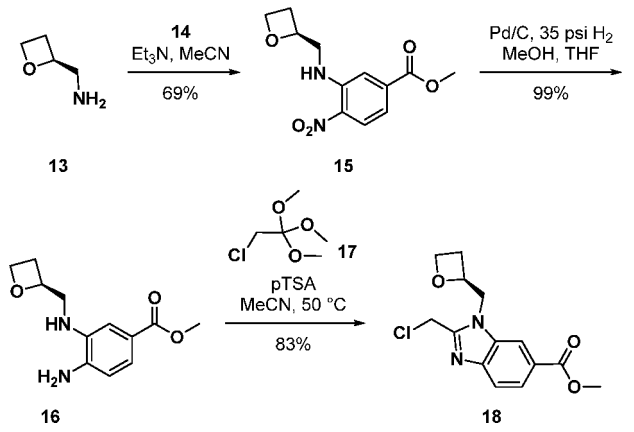

reagent allowed for selective saponification of the ester to predominate over competing hydrolysis of the 4-cyano group.

A solution of danuglipron in warm 1-propanol was treated with an aqueous solution of tris(hydroxymethyl)aminomethane. The mixture was seeded, cooled to room temperature, and stirred for 15 h. Crystalline danuglipron, Tris salt was collected by filtration and dried under reduced pressure.

The synthesis and characterization of other analogues are provided in the Supporting Information.

CONCLUSIONS

In summary, we developed a novel sensitized HTS assay that identified a series of small-molecule GLP-1R agonists. The series was optimized for pharmacologic potency, safety, and disposition attributes amenable for use in humans. Danuglipron demonstrated an *in vitro* signaling profile similar to that of GLP-1, potentiated glucose-stimulated insulin release, decreased the rate of food intake in monkeys, and was orally available in healthy human participants. Furthermore, danuglipron demonstrated beneficial changes during a recently reported multiple-dose study in volunteers with T2DM.[52] This

Scheme 3. Synthesis of Danuglipron

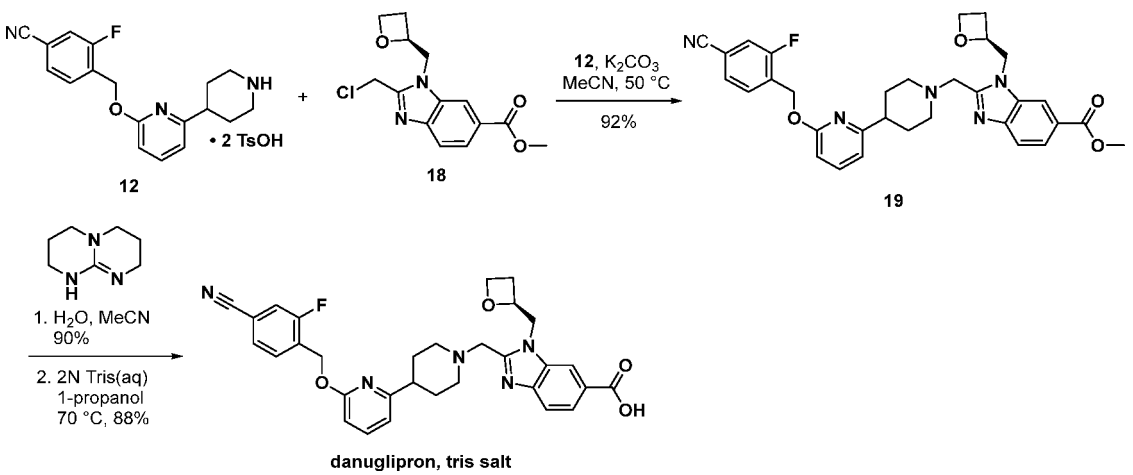

https://doi.org/10.1021/acs.jmedchem.1c01856
J. Med. Chem. 2022, 65, 8208−8226

research had a number of strengths, including the demonstration that a PAM-sensitized SA could identify very weak hits for a challenging GPCR target. The iterative process of discovery and development of danuglipron from weak hits through to demonstration of the compound's bioavailability in humans is described, highlighting the multiple considerations taken when designing and selecting an optimal drug candidate. That such low-molecular weight agonists can recapitulate the pharmacology of the peptide GLP-1R agonists sheds further light on this important therapeutic target. To the best of our knowledge, this is the first literature report of decreasing glucose levels with an oral small-molecule agonist of the GLP-1R in humans.

EXPERIMENTAL SECTION

Unless otherwise stated, all reactants, reagents, and solvents were obtained from commercial sources and used without further purification. All compounds are >95% pure as determined by HPLC analysis. Data for ^{1}H nuclear magnetic resonance (NMR) spectra, obtained with a spectrometer at 600 or 400 MHz, are reported relative to residual solvent signals (for $CDCl_3$, δH = 7.27 ppm; for DMSO-d_6, δH = 2.50 ppm; for CD_3OD, δH = 3.31 ppm) as follows: chemical shift (δ, parts per million), multiplicity, coupling constant (hertz) and integration. The multiplicities are denoted as follows: s, singlet; d, doublet; t, triplet; q, quartet; spt, septet; m, multiplet; br s, broad singlet. Data for ^{13}C NMR spectra are reported in terms of chemical shift (δ) relative to residual solvent signals (for $CDCl_3$, δC = 77.0 ppm; for DMSO-d_6, δC = 39.5 ppm; for CD_3OD, δC = 49.2 ppm). Flash chromatography was carried out on either a Biotage SP purification system or a Combiflash Companion from Teledyne Isco; Biotage SNAP, KPsil, or Redisep Rf silica columns were used. Reaction mixtures were magnetically stirred, and reactions monitored by thin layer chromatography, liquid chromatography–mass spectrometry (LCMS), and/or high-performance liquid chromatography (HPLC). Except where otherwise noted, all reactions were run under an inert atmosphere of nitrogen gas using anhydrous solvents at room temperature (~23 °C). The terms "concentrated" and "evaporated" refer to the removal of solvent at reduced pressure on a rotary evaporator with a water bath temperature not exceeding 60 °C. All compounds evaluated were >95% pure.

Cell Line Generation. The human GLP-1R (reference sequence NM_002062) cDNA was amplified by RT-PCR and subcloned into pcDNA3.1 and pcDNA5/FRT/TO (Thermo Fisher, Pittsburgh, PA). CHO-K1 cells (ATCC) were transfected with pcDNA3.1/GLP-1R, and a clonal cell line with high receptor expression levels was selected for membrane preparations to support binding studies ("binding cell line"). The pcDNA5/FRT/TO/GLP-1R plasmid was transfected into the Flp-In-CHO cell line (Thermo Fisher), and clonal cell lines with medium receptor levels ("SA cell line") and lower receptor levels ("CS cell line") were selected. High-, medium-, and low-expression cell lines were selected on the basis of receptor mRNA expression levels (qPCR) and cAMP responses to GLP-1 and were utilized for lead identification and SAR efforts, as indicated. A procedure similar to that used to create the "SA cell line" was used to generate CHO cells stably expressing the mouse (NM_021332.2) and cynomolgus (NM_001287663.1) GLP-1R.

Compound Synthesis. See the Supplementary Methods for detailed descriptions of compound synthesis.

cAMP Production Assays for SAR. CHO-K1 cells stably expressing the human GLP-1R (either the screening cell line or the CS cell line, as noted in the text) were removed from cryopreservation, thawed, centrifuged (1000 rpm, 5 min), and resuspended in complete cell culture medium (Dulbecco's modified Eagle's medium F12, 10% heat-inactivated fetal bovine serum, 500 μg/mL geneticin, 50 units/mL penicillin, 50 μg/mL streptomycin, and 2 mM glutamine). Cells were plated at a density of 1600 cells/well (50 μL/well) into Corning 3570 assay plates (Fisher Scientific) and cultured for 48 h in a humidified environment at 37 °C with 5% CO_2. On the day of the assay, compounds were serially diluted by half-logs in DMSO as an 11-point concentration response and added in 1 μL per well in 384-well polypropylene plates to create intermediate plates. The intermediate plates were then diluted with 100 μL/well of assay buffer (Hanks balanced salt solution with calcium and magnesium, 10 mM HEPES, 0.1% bovine serum albumin, and 100 μM IBMX). For BETP-sensitized assays, a concentration of 3 μM was added to the assay buffer. Positive control wells containing 1 μM GLP-1 (final concentration) and negative control wells containing 1% DMSO (final concentration) were included on all plates. The cell culture medium was removed from the cell plates, and 20 μL of the diluted compounds was transferred to the cells. Assay plates were then incubated for 30 min in a humidified environment at 37 °C with 5% CO_2. The production of cAMP was measured using the HI Range cAMP detection kit (Cisbio, Bedford, MA) according to the manufacturer's instructions. The cAMP-d2 working solution was added to the assay plates in portions of 10 μL per well followed by 10 μL of an anti-cAMP-cryptate working solution. Assay plates were incubated for 1 h at room temperature on the lab bench, and the fluorescence was read using an EnVision plate reader (PerkinElmer, Chicago, IL) with excitation at 330 nm and emissions of 615 and 665 nm. A cAMP standard curve was used to convert the raw data (ratio of the 665 and 615 nm reads) to cAMP concentrations, as recommended by the manufacturer. The interpolated data (cAMP concentrations) were analyzed using Activity Base (IDBS). The percent effect at each concentration of compound was calculated by Activity Base relative to the amount of cAMP in the positive and negative control wells on each assay plate. Compound EC_{50} values were determined using a logistic four-parameter fit model. The E_{max} for each compound was defined by the maximum asymptote of the fitted curve and expressed as a percent of the maximum response produced by the positive control on each plate.

BETP-Sensitized cAMP HTS Assay. The HTS utilized the Cisbio cAMP homogeneous time-resolved fluorescence assay technology. CHO-K1 cells stably expressing the human GLP-1R (screening cell line) were removed from cryopreservation, thawed, centrifuged (1000 rpm, 5 min), and resuspended in complete cell culture medium [Dulbecco's modified Eagle's medium F12, 10% heat-inactivated fetal bovine serum, 500 μg/mL Geneticin (G418), 50 units/mL penicillin, 50 μg/mL streptomycin, and 2 mM glutamine]. Cells were plated at a density of 1500 cells/well (20 μL/well) on 384-well assay plates and cultured for 48 h in a humidified environment at 37 °C with 5% CO_2. A library of approximately 2.8 million compounds from the Pfizer Sample Bank was screened in a compressed format, with 14 compounds per well, each at a final assay concentration of 10 μM. On the day of the assay, compounds were added in portions of 1 μL per well in 384-well polypropylene plates to create intermediate plates. The intermediate plates were then diluted with 100 μL of assay buffer [Hanks balanced salt solution (HBSS) with calcium and magnesium, 10 mM HEPES, 0.1% bovine serum albumin, 100 μM IBMX, and 3 μM BETP] per well. Positive control wells containing 100 nM GLP-1(7–36)amide (GLP-1; final concentration) and negative control wells containing 1% DMSO (final concentration) were included on all plates. The cell culture medium was removed from the cell plates, and 20 μL of the diluted compounds was transferred to the cells. Assay plates were then incubated for 30 min in a humidified environment at 37 °C with 5% CO_2. The production of cAMP was measured using the HI Range cAMP detection kit (Cisbio) according to the manufacturer's instructions. The cAMP-d2 working solution was added to the assay plates in portions of 10 μL per well followed by 10 μL of an anti-cAMP-cryptate working solution. Assay plates were incubated for 1 h at room temperature, and the fluorescence was read using an EnVision plate reader (PerkinElmer) with excitation at 330 nm and emissions of 615 and 665 nm. A cAMP standard curve was used to convert the raw data (ratio of the 665 and 615 nm reads) to cAMP concentrations, as recommended by the manufacturer. The interpolated data (cAMP concentrations) were analyzed using Activity Base (IDBS). The percent effect at each concentration of compound was calculated by

https://doi.org/10.1021/acs.jmedchem.1c01856
J. Med. Chem. 2022, 65, 8208–8226

Activity Base relative to the amount of cAMP in the positive and negative control wells on each assay plate.

βArr Recruitment Assay (assay medium). βArr recruitment at the human GLP-1R was evaluated using DiscoverX's enzyme fragment complementation technology as described by the manufacturer (DiscoverX, Fremont, CA). Cryopreserved Path Hunter GLP-1 βArr1- or βArr2-expressing cells were thawed, washed, and resuspended in complete growth medium (HAMs/F-12 medium containing 10% heat-inactivated FBS, 1× Pen/Strep, 1× glutamine, 300 μg/mL hygromycin, and 800 μg/mL geneticin). Following overnight incubation at 37 °C in a humidified environment (5% CO_2), cells were dissociated and replated in white 384-well plates at a density of 5000 cells/well in 18 μL of assay medium overnight (HAMs/F-12 medium containing 10% heat-inactivated FBS, 1× Pen/Strep, and 1× glutamine).

Compounds were serially diluted as 11-point, half-log dose responses in 100% DMSO, and 1 μL of the serially diluted compounds was transferred to a compound source plate. Prior to addition to cells, the 1 μL compound spots were diluted in assay medium with or without BETP. Two microliters of a 20× compound dose−response series was transferred from the compound source plate to the appropriate well in the assay plate. The final BETP concentration of wells containing BETP was 10 μM. Plates were then incubated with the compound for 90 min at 37 °C in a humidified environment (5% CO_2). Following the 90 min incubation, 10 μL of Path Hunter Detection Reagent was added per well and assay plates were incubated for 60 min at room temperature. Chemiluminescence activity was then measured using an EnVision multilabel plate reader.

The raw data were analyzed using Activity Base (IDBS). The percent effect at each compound concentration was calculated in Activity Base, relative to the positive and negative control wells on each assay plate. The negative control wells contained a final assay concentration of 1% DMSO, while the positive control wells contained a final assay concentration of 1 μM GLP-1. Compound EC_{50} values were determined using a logistic four-parameter fit model. The E_{max} for each compound was defined by the maximum asymptote of the fitted curve and expressed as a percent of the maximum response produced by the plated positive control.

See the Supplementary Methods for details about how additional assays in this study were performed.

Animal Pharmacokinetic Studies. Jugular vein/carotid artery doubly cannulated male Wistar-Han rats (~250 g), obtained from Charles River Laboratories (Wilmington, MA), and male cynomolgus monkeys (~7 kg) were used for these studies. Animals were fasted overnight and through the duration of the study (1.0 or 2.0 h), whereas access to water was provided *ad libitum*. Danuglipron was administered by slow iv bolus as a solution (1 mg/mL) in a 5:95 (v/v) polyethylene glycol 400/12% (w/v) sulfobutyl-β-cyclodextrin in water mixture or a 10:50:40 (v/v/v) DMSO/polyethylene glycol 400/water mixture via the tail vein in rats (n = 4) or the femoral vein in monkeys (n = 2) at a dose of 1.0 mg/kg in a dosing volume of 1 mL/kg. Serial blood samples were collected before dosing and 0.083, 0.25, 0.5, 1.0, 2.0, 4.0, 7.0, and 24 h after dose administration. The crystalline 2-amino-2-hydroxymethylpropane-1,3-diol (Tris) salt form of danuglipron was also administered by oral gavage to rats (5 and 100 mg/kg at 10 mL/kg) and monkeys [5 mg/kg (5.0 mL/kg) and 100 mg/kg (10 mL/kg)] as a homogeneous suspension in a 2:98 (v/v) Tween 80/0.5% (w/v) methylcellulose A4M in distilled water mixutre. Blood samples were taken prior to po administration, and then serial samples were collected 0.083, 0.25, 0.5, 1, 2, 4, 7, and 24 h after dosing. Blood samples from the pharmacokinetic studies were centrifuged to generate plasma. All plasma samples were kept frozen until analysis. For rat and monkey samples, aliquots of plasma (20−50 μL) were transferred to 96-well blocks, and acetonitrile (150−200 μL) containing verapamil (monkeys) or terfenadine (rat) as internal standard was added to each well. The supernatant was dried under nitrogen and reconstituted with 100 μL of water without evaporation. Following extraction, the samples were then analyzed by liquid chromatography tandem mass spectrometry (LC-MS/MS), and concentrations of danuglipron in plasma were determined by interpolation from a standard curve as described in the Supporting Information.

Determination of Preclinical Pharmacokinetic Parameters. Pharmacokinetic parameters in animals were determined using noncompartmental analysis (Watson version 7.4, Thermo Scientific, Waltham, MA). Maximum plasma concentrations (C_{max}) of danuglipron in plasma after po dosing in rats and monkeys were determined directly from the experimental data, with T_{max} defined as the time of first occurrence of C_{max}. The area under the plasma concentration−time curve from time zero to infinity ($AUC_{0-\infty}$) was estimated using the linear trapezoidal rule. Systemic plasma clearance (CL_p) was calculated as the intravenous dose divided by $AUC_{0-\infty}^{iv}$. The terminal rate constant (k_{el}) was calculated by a linear regression of the log-linear concentration−time curve, and the terminal elimination $t_{1/2}$ was calculated as $0.693/k_{el}$. The apparent steady-state distribution volume (Vd_{ss}) in animals was determined as the iv or po dose divided by the product of $AUC_{0-\infty}$ and k_{el}. The absolute bioavailability (F) of the po doses in animals was calculated using the equation $F = AUC_{0-\infty}^{po}/AUC_{0-\infty}^{iv} \times dose^{iv}/dose^{po}$.

Detailed protocols used in animal pharmacology studies are provided in the Supplementary Methods.

Phase 1 Clinical Study. The safety, tolerability, and pharmacokinetics of danuglipron were evaluated in a first-in-human, Phase 1, randomized, double-blind, placebo-controlled, single ascending dose study in healthy adult participants (NCT03309241). A total of 25 participants were randomized. Each participant received up to four single oral doses of danuglipron (immediate release tablets) and up to two placebo doses. In a given participant, there was an interval of at least 7 days between consecutive study periods to allow for washout of danuglipron and review safety and pharmacokinetic data from each dose level before decisions were made on the next dose. Participants who discontinued for non-safety-related reasons prior to completion of the study may have been replaced at the discretion of the principal investigator and sponsor. The starting dose of 3 mg was derived from nonclinical information about the pharmacokinetics and metabolism of danuglipron. Blood samples for safety (including fasting serum glucose) and pharmacokinetic assessments were collected 0, 0.3, 0.75, 1.25, 2, 3, 4, 6, 8, 10, 12, 24, 26, and 48 h after the dose.

All observed and self-reported AEs, any clinically significant changes in physical examination results, and abnormal test results were recorded. Laboratory evaluations included hematology, chemistry, and urinalysis. Twelve-lead electrocardiogram and vital signs were monitored throughout.

Additional details are available in the Supplementary Methods.

Synthesis of Danuglipron. *1-(tert-Butyl) 4-Methyl 4-(6-chloropyridin-2-yl)piperidine-1,4-dicarboxylate (**8**).* To a stirred solution of 1-(*tert*-butyl)-4-methyl piperdine-1,4-dicarboxylate (**7**, 1.68 mL, 6.2 mmol) and 2,6-dichloropyridine (**6**, 0.82 g, 5.5 mmol) in $PhCH_3$ (5.5 mL) was added lithium bis(trimethylsilyl)amide (LiHMDS) in THF (1 M, 7.2 mL). After 15 h, the solution was acidified with HCl in water (0.5 N, 15 mL). The aqueous phase was extracted with EtOAc (2 × 25 mL), and the combined organic layers were dried over anhydrous Na_2SO_4, filtered, and evaporated under reduced pressure to give a colorless oil. The crude material was purified using column chromatography eluting with 20% EtOAc in heptane to afford 1-(*tert*-butyl) 4-methyl 4-(6-chloropyridin-2-yl)-piperidine-1,4-dicarboxylate (**8**) as a colorless oil (0.87 g, 45%): ^{1}H NMR (600 MHz, $CDCl_3$) δ 7.62 (t, J = 7.9 Hz, 1H), 7.21 (d, J = 7.6 Hz, 2H), 3.83 (br s, 2H), 3.71 (s, 3H), 3.14 (br s, 2H), 2.41 (d, J = 13.5 Hz, 2H), 2.08 (ddd, J = 13.6, 10.4, 3.5 Hz, 2H), 1.45 (s, 9H); MS (ES) m/z 255.2 $(M - Boc + H)^+$.

*tert-Butyl 4-(6-Chloropyridin-2-yl)piperidine-1-carboxylate (**9**).* To a stirred solution of 1-(*tert*-butyl) 4-methyl 4-(6-chloropyridin-2-yl)piperidine-1,4-dicarboxylate (**8**, 0.87 g, 2.4 mmol) in MeOH (10 mL) was added NaOH in water (2 N, 6 mL) at 60 °C. After 5 h, the solution was allowed to cool to room temperature and acidified with HCl in water (1 N, 50 mL). The aqueous phase was extracted with EtOAc (3 × 75 mL), and the combined organic layers were dried over anhydrous Na_2SO_4, filtered, and evaporated under reduced pressure to give a white solid. The crude material was dissolved in DCE (24

https://doi.org/10.1021/acs.jmedchem.1c01856
J. Med. Chem. 2022, 65, 8208−8226

mL) and stirred at reflux. After 2 h, the mixture was concentrated and treated with 25% water in MeOH (4 mL). After 4 h, the resultant solid was filtered and dried under reduced pressure to afford *tert*-butyl 4-(6-chloropyridin-2-yl)piperidine-1-carboxylate (**9**) as a white solid (0.64 g, 88%): ^{1}H NMR (600 MHz, $CDCl_3$) δ 7.58 (t, J = 7.6 Hz, 1H), 7.17 (d, J = 8.2 Hz, 1H), 7.06 (d, J = 7.6 Hz, 1H), 4.25 (br s, 2H), 2.93−2.66 (m, 3H), 1.91 (d, J = 12.9 Hz, 2H), 1.69 (qd, J = 12.5, 4.1 Hz, 2H), 1.47 (s, 9H); MS (ES) m/z 241.2 $(M - tBu)^+$.

*tert-Butyl 4-{6-[(4-Cyano-2-fluorobenzyl)oxy]pyridin-2-yl}-piperidine-1-carboxylate (**11**).* A reaction vessel equipped with a reflux condenser was charged with *tert*-butyl 4-(6-chloropyridin-2-yl)piperidine-1-carboxylate (**9**, 3.0 g, 10.1 mmol), 3-fluoro-4-(hydroxymethyl)benzonitrile (**10**, 1.6 g, 10.6 mmol), $Pd(OAc)_2$ (0.11 g, 0.51 mmol), (*S*)-2-(di-*tert*-butylphosphino)-1,1′-binaphthyl (Trixiephos, 0.20 g, 0.51 mmol), and Cs_2CO_3 (6.8 g, 21 mmol). 1,4-Dioxane (51 mL) was added, and the mixture was heated to 105 °C. After 2 h, the mixture was allowed to cool to room temperature, filtered through a plug of silica gel and Celite, and eluted with a 50:50 mixture of EtOAc and heptanes (200 mL), and the filtrate was evaporated under reduced pressure. The crude material was purified using column chromatography eluting with EtOAc in heptane (10:90 to 25:75) to obtain *tert*-butyl 4-{6-[(4-cyano-2-fluorobenzyl)oxy]-pyridin-2-yl}piperidine-1-carboxylate (**11**) as an off-white solid (3.8 g, 91%): ^{1}H NMR (600 MHz, $CDCl_3$) δ 7.62 (t, J = 7.3 Hz, 1H), 7.53 (t, J = 7.9 Hz, 1H), 7.44 (d, J = 7.6 Hz, 1H), 7.37 (d, J = 9.4 Hz, 1H), 6.75 (d, J = 7.0 Hz, 1H), 6.65 (d, J = 8.2 Hz, 1H), 5.49 (s, 2H), 4.20 (br s, 2H), 2.81 (br s, 2H), 2.70 (tt, J = 11.7, 3.5 Hz, 1H), 1.82 (d, J = 12.9 Hz, 2H), 1.67 (d, J = 11.2 Hz, 2H), 1.49 (s, 9H); MS (ES^+) 356.2 $(M - tBu)^+$.

*3-Fluoro-4-({[6-(piperidin-4-yl)pyridin-2-yl]oxy}methyl)-benzonitrile (**12**).* To a stirred solution of *tert*-butyl 4-{6-[(4-cyano-2-fluorobenzyl)oxy]pyridin-2-yl}piperidine-1-carboxylate (**11**, 102 g, 242 mmol) in EtOAc (1350 mL) was added pTSA monohydrate (120 g, 630 mmol). The mixture was heated to 60 °C. After 15 min, the solution was allowed to cool to room temperature and the resultant solid was filtered and dried under reduced pressure to afford 3-fluoro-4-({[6-(piperidin-4-yl)pyridin-2-yl]oxy}methyl)benzonitrile bis-pTSA salt (**12**, 149 g, 94%) as a white solid: ^{1}H NMR (600 MHz, DMSO-d_6) δ 8.53 (br s, 1H), 8.26 (br s, 1H), 7.89 (d, J = 10.0 Hz, 1H), 7.78−7.67 (m, 3H), 7.48 (d, J = 8.2 Hz, 4H), 7.11 (d, J = 7.6 Hz, 4H), 6.90 (d, J = 7.0 Hz, 1H), 6.79 (d, J = 8.2 Hz, 1H), 5.48 (s, 2H), 3.35 (d, J = 12.3 Hz, 2H), 3.09−2.96 (m, 2H), 2.96−2.79 (m, 1H), 2.29 (s, 6H), 2.03−1.93 (m, 2H), 1.90−1.77 (m, 2H); MS(ES) m/z 312.5 $(M + H)^+$.

*Methyl (S)-4-Nitro-3-[(oxetan-2-ylmethyl)amino]benzoate (**15**).* To a stirred solution of methyl-3-fluoro-4-nitrobenzoate (**14**, 0.38 g, 4.4 mmol) in MeCN (25 mL) was added (*S*)-oxetan-2-ylmethanamine (**13**, 1.0 g, 5.2 mmol[53]), followed by Et_3N (1.8 mL, 13.1 mmol). After 18 h, the reaction mixture was concentrated *in vacuo* and treated with saturated NH_4Cl (15 mL). The aqueous phase was extracted with EtOAc (3 × 25 mL), and the combined organic layers were dried over anhydrous Na_2SO_4, filtered, and evaporated under reduced pressure. The crude material was purified using column chromatography eluting with EtOAc in heptane (0:100 to 40:60) to afford methyl (*S*)-4-nitro-3-[(oxetan-2-ylmethyl)amino]benzoate (**15**, 0.81 g, 69%) as an orange solid: ^{1}H NMR (600 MHz, $CDCl_3$) δ 8.37 (br s, 1H), 8.25 (d, J = 8.8 Hz, 1H), 7.64 (s, 1H), 7.28 (d, J = 8.8 Hz,1H), 5.22−5.12 (m, 1H), 4.76 (q, J = 7.5 Hz, 1H), 4.64 (dt, J = 5.9, 9.2 Hz, 1H), 3.95 (s, 3H), 3.64 (t, J = 4.3 Hz, 2H), 2.84−2.75 (m, 1H), 2.66−2.57 (m, 1H); MS(ES) m/z 242.4 $(M - 24)^+$.

*(S)-4-Amino-3-[(oxetan-2-ylmethyl)amino]benzoate (**16**).* To a stirred solution of methyl (*S*)-4-nitro-3-[(oxetan-2-ylmethyl)amino]-benzoate (**15**, 1.4 g, 5.4 mmol) in MeOH (120 mL) and THF (20 mL) was added Pd/C [10% (w/w), 0.42 g, 0.22 mmol]. The solution was subjected to a hydrogen atmosphere (35 PSI) at room temperature. After 4 h, the solution was filtered through a Celite plug, washed with MeOH (2 × 25 mL), and concentrated under reduced pressure to provide (*S*)-4-amino-3-[(oxetan-2-ylmethyl)-amino]benzoate (**16**, 1.3 g, >99%) as a beige oil: ^{1}H NMR (600 MHz, $CDCl_3$) δ 7.49 (d, 1H), 7.39 (s, 1H), 6.70 (d, J = 7.9 Hz, 1H), 5.16−5.08 (m, 1H), 4.76 (q, J = 6.2, 9.1 Hz, 1H), 4.62 (q, J = 6.2, 9.1 Hz, 1H), 3.87 (br s, 5H), 3.54 (br s, 1H), 3.45 (q, J = 5.9, 12.3 Hz, 1H), 3.40−3.34 (m, 1H), 2.83−2.73 (m, 1H), 2.66−2.56 (m, 1H); MS(ES) m/z 237.2 $(M + H)^+$.

*(S)-2-(Chloromethyl)-1-(oxetan-2-ylmethyl)-1H-benzo[d]-imidazole-6-carboxylate (**18**).* To a stirred solution of methyl (*S*)-4-amino-3-[(oxetan-2-ylmethyl)amino]benzoate (**16**, 3.0 g, 12.7 mmol) in THF (51 mL) was added 2-chloro-1,1,1-trimethoxyethane (**17**, 1.9 mL, 14 mmol) followed by pTSA monohydrate (0.13 g, 0.67 mmol). The mixture was heated to 40 °C. After 1.5 h, the reaction mixture was concentrated *in vacuo* and azetroped with a 50:50 mixture of EtOAc and heptanes (50 mL) to provide an orange solid. The solid was treated with EtOAc (25 mL), heated to 50 °C, diluted with heptane (140 mL), and allowed to cool to room temperature. After 2 h, the mixture was filtered, washed with heptane (2 × 10 mL), and dried to provide (*S*)-2-(chloromethyl)-1-(oxetan-2-ylmethyl)-1*H*-benzo[*d*]imidazole-6-carboxylate (**18**, 3.1 g, 83%) as an off-white solid: ^{1}H NMR (600 MHz, $CDCl_3$) δ 8.13 (s, 1H), 8.02 (d, J = 8.5 Hz, 1H), 7.81 (d, J = 8.5 Hz, 1H), 5.22 (dq, J = 2.6, 6.9 Hz, 1H), 5.05 (s, 2H), 4.66−4.60 (m, 2H), 4.57−4.52 (m, 1H), 4.35 (td, J = 6.0, 9.1 Hz, 1H), 3.97 (s, 3H), 2.82−2.73 (m, 1H), 2.48−2.39 (m, 1H); MS(AP) m/z 295.2 $(M + H)^+$.

*(S)-2-[(4-{6-[(4-Cyano-2-fluorobenzyl)oxy]pyridin-2-yl}piperidin-1-yl)methyl]-1-(oxetan-2-ylmethyl)-1H-benzo[d]imidazole-6-carboxylate (**19**).* To a stirred solution of methyl (*S*)-2-(chloromethyl)-1-(oxetan-2-ylmethyl)-1*H*-benzo[*d*]imidazole-6-carboxylate (**18**, 1.8 g, 6.1 mmol) in MeCN (35 mL) were added 3-fluoro-4-({[6-(piperidin-4-yl)pyridin-2-yl]oxy}methyl)benzonitrile bis-pTSA salt (**12**, 4.1 g, 6.1 mmol) and K_2CO_3 (4.2 g, 30.4 mmol). The heterogeneous mixture was heated to 50 °C. After 2 h, the solution was treated with water (70 mL), allowed to cool to room temperature, and stirred for 2 h. The mixture was filtered, washed with water (2 × 30 mL), and dried under reduced pressure to provide (*S*)-2-[(4-{6-[(4-cyano-2-fluorobenzyl)oxy]pyridin-2-yl}piperidin-1-yl)methyl]-1-(oxetan-2-ylmethyl)-1*H*-benzo[*d*]imidazole-6-carboxylate (**19**, 3.2 g, 92%) as a white solid: ^{1}H NMR (600 MHz, $CDCl_3$) δ 8.19 (s, 1H), 7.98 (d, J = 8.6 Hz, 1H), 7.76 (d, J = 8.6 Hz, 1H), 7.63 (t, J = 7.6 Hz, 1H), 7.53 (t, J = 7.6 Hz, 1H), 7.45 (d, J = 8.2 Hz, 1H), 7.38 (d, J = 9.8 Hz, 1H), 6.76 (d, J = 7.4 Hz, 1H), 6.65 (d, J = 8.2 Hz, 1H), 5.51 (s, 2H), 5.29−5.19 (m, 1H), 4.81−4.68 (m, 2H), 4.67−4.60 (m, 1H), 4.42 (td, J = 6.0, 9.1 Hz, 1H), 3.97 (s, 2H), 3.96 (s, 3H), 3.04−2.92 (m, 2H), 2.81−2.69 (m, 1H), 2.67−2.55 (m, 1H), 2.54−2.42 (m, 1H), 2.35−2.21 (m, 2H), 1.93−1.72 (m, 4H); MS(AP) m/z 570.5 $(M + H)^+$.

(S)-2-[(4-{6-[(4-Cyano-2-fluorobenzyl)oxy]pyridin-2-yl}piperidin-1-yl)methyl]-1-(oxetan-2-ylmethyl)-1H-benzo[d]imidazole-6-carboxylic Acid (danuglipron). To a stirred solution of methyl (*S*)-2-[(4-{6-[(4-cyano-2-fluorobenzyl)oxy]pyridin-2-yl}piperidin-1-yl)-methyl]-1-(oxetan-2-ylmethyl)-1*H*-benzo[*d*]imidazole-6-carboxylate (**19**, 4 g, 7 mmol) in MeCN (70 mL) was added a solution of 1,5,7-triazabicyclo[4.4.0]dec-5-ene in water (TBD, 0.97 M, 14.7 mL, 14.4 mmol). After 24 h, the solution was acidified to pH ∼4.5 with citric acid in water (1 N, 14 mL) and diluted with water (50 mL). The aqueous phase was extracted with EtOAc (2 × 75 mL), and the combined organic layers were dried over anhydrous Na_2SO_4, filtered, and evaporated under reduced pressure to give an off-white solid. The crude material was purified using column chromatography eluting with a MeOH/DCM mixture (0:100 to 8:92) to afford (*S*)-2-[(4-{6-[(4-cyano-2-fluorobenzyl)oxy]pyridin-2-yl}piperidin-1-yl)methyl]-1-(oxetan-2-ylmethyl)-1*H*-benzo[*d*]imidazole-6-carboxylic acid (danuglipron, 3.65 g, 90%) as a white amorphous solid: ^{1}H NMR (400 MHz, DMSO-d_6) δ 12.75 (br s, 1H), 8.27 (s, 1H), 7.89 (d, J = 10.1 Hz, 1H), 7.80 (d, J = 9.4 Hz, 1H), 7.72−7.68 (m, 2H), 7.67−7.60 (m, 2H), 6.89 (d, J = 7.4 Hz, 1H), 6.72 (d, J = 8.2 Hz, 1H), 5.47 (s, 2H), 5.11 (d, J = 3.9 Hz, 1H), 4.86−4.74 (m, 1H), 4.72−4.62 (m, 1H), 4.53−4.43 (m, 1H), 4.35−4.32 (m, 1H), 3.95 (d, J = 13.7 Hz, 1H), 3.77 (d, J = 13.7 Hz, 1H), 2.98 (d, J = 10.1 Hz, 1H), 2.84 (d, J = 11.7 Hz, 1H), 2.77−2.65 (m, 1H), 2.64−2.53 (m, 1H), 2.45−2.37 (m, 1H), 2.28−2.10 (m, 2H), 1.84−1.57 (m, 4H); MS(ES) m/z 556.6 $(M + H)^+$.

https://doi.org/10.1021/acs.jmedchem.1c01856
J. Med. Chem. 2022, 65, 8208−8226

(S)-2-[(4-{6-[(4-Cyano-2-fluorobenzyl)oxy]pyridin-2-yl}piperidin-1-yl)methyl]-1-(oxetan-2-ylmethyl)-1H-benzo[d]imidazole-6-carboxylic Acid (danuglipron, Tris salt). To a stirred solution of (*S*)-2-[(4-{6-[(4-cyano-2-fluorobenzyl)oxy]pyridin-2-yl}piperidin-1-yl)-methyl]-1-(oxetan-2-ylmethyl)-1*H*-benzo[*d*]imidazole-6-carboxylic acid (danuglipron, 6.5 g, 11.7 mmol) in 1-propanol (275 mL) at 70 °C was added a solution of tris(hydroxymethyl)aminomethane in water (2 M, 6.1 mL, 12.2 mmol) dropwise. The homogeneous solution was seeded, allowed to cool to room temperature over 2 h, and stirred for 15 h. The mixture was filtered, washed with 1-propanol (2 × 30 mL), and dried under reduced pressure to provide (*S*)-2-[(4-{6-[(4-cyano-2-fluorobenzyl)oxy]pyridin-2-yl}piperidin-1-yl)methyl]-1-(oxetan-2-ylmethyl)-1*H*-benzo[*d*]imidazole-6-carboxylic acid (danuglipron, Tris salt, 7.0 g, 88%) as a white crystalline solid: ^{1}H NMR (400 MHz, DMSO-d_6) δ 8.20 (s, 1H), 7.89 (d, J = 9.8 Hz, 1H), 7.79 (d, J = 8.3 Hz, 1H), 7.70 (br s, 2H), 7.64 (t, J = 7.8 Hz, 1H), 7.55 (d, J = 8.3 Hz, 1H), 6.88 (d, J = 7.3 Hz, 1H), 6.72 (d, J = 8.3 Hz, 1H), 5.47 (s, 2H), 5.15−5.06 (m, 1H), 4.84−4.73 (m, 1H), 4.72−4.59 (m, 1H), 4.53−4.44 (m, 1H), 4.38 (dt, J = 6.0, 8.8 Hz, 1H), 3.93 (d, J = 13.4 Hz, 1H), 3.76 (d, J = 13.4 Hz, 1H), 3.36 (s, 9H), 2.98 (d, J = 11.0 Hz, 1H), 2.85 (d, J = 11.0 Hz, 1H), 2.77−2.64 (m, 1H), 2.63−2.53 (m, 1H), 2.47−2.40 (m, 1H), 2.26−2.11 (m, 2H), 1.82−1.56 (m, 4H); ^{13}C NMR (101 MHz, DMSO-d_6, ^{1}H and ^{19}F decoupled) δ 169.7, 162.4, 161.6, 159.6, 153.6, 143.9, 139.9, 135.6, 131.2, 131.0, 129.7, 128.7, 123.0, 119.2, 117.6, 114.6, 112.3, 112.0, 108.1, 80.6, 67.6, 61.1, 60.0, 59.2, 55.1, 53.7, 53.2, 48.9, 42.8, 31.2, 31.1, 24.5; ^{13}C NMR (101 MHz, DMSO-d_6, ^{1}H decoupled, just J_{sp^2C-F} reported) δ 159.5 (d, J = 248.5 Hz), 133.6 (d, J = 4.5 Hz), 131.0 (d, J = 14.6 Hz), 128.7 (d, J = 3.5 Hz), 119.2 (d, J = 25.6 Hz), 117.5 (d, J = 2.5 Hz), 112.0 (d, J = 10 Hz); ^{19}F NMR (376 MHz, DMSO-d_6) δ −115.5; HRMS (ESI) m/z $[M + H]^+$ for $C_{31}H_{30}FN_5O_4$ calcd 556.2350, found 556.2334; mp 194 °C.

■ ASSOCIATED CONTENT

Supporting Information

The Supporting Information is available free of charge at https://pubs.acs.org/doi/10.1021/acs.jmedchem.1c01856.

Tables S1−S7 with supporting GLP-1R pharmacology data and off-target pharmacology data; Figures S1−S3 with signaling bias, FAP-tagged human GLP-R cAMP data, and published structures supporting residue 33 extending toward solvent, respectively; syntheses of compounds **1**−**5** and PF-06883365; NMR spectra; HPLC traces; plasma membrane isolations; radioligand binding assay methods; off-target selectivity assessments; several functional assays; bias calculations; confocal microscopy; functional assessments; cryo-EM methods; animal studies; study design for the first-in-human study; and supplementary references (PDF)

PDB validation report for the GLP-1R complexed with PF-06883365 [PDB entry 7S15 (Figure 4)] (PDF)

Molecular formula strings (CSV)

Accession Codes

EM density map and atomic coordinates for the GLP-1R complexed with PF-06883365 are accessible through EMD entry 24794 and PDB entry 7S15 (Figure 4).

■ AUTHOR INFORMATION

Corresponding Author

David A. Griffith − *Pfizer Worldwide Research, Development, and Medical, Cambridge, Massachusetts 02139, United States;* orcid.org/0000-0002-7592-2478; Email: david.a.griffith@pfizer.com

Authors

David J. Edmonds − *Pfizer Worldwide Research, Development, and Medical, Cambridge, Massachusetts 02139, United States*

Jean-Philippe Fortin − *Pfizer Worldwide Research, Development, and Medical, Cambridge, Massachusetts 02139, United States*

Amit S. Kalgutkar − *Pfizer Worldwide Research, Development, and Medical, Cambridge, Massachusetts 02139, United States;* orcid.org/0000-0001-9701-756X

J. Brent Kuzmiski − *Pfizer Worldwide Research, Development, and Medical, Cambridge, Massachusetts 02139, United States*

Paula M. Loria − *Pfizer Worldwide Research, Development, and Medical, Groton, Connecticut 06340, United States*

Aditi R. Saxena − *Pfizer Worldwide Research, Development, and Medical, Cambridge, Massachusetts 02139, United States*

Scott W. Bagley − *Pfizer Worldwide Research, Development, and Medical, Groton, Connecticut 06340, United States;* orcid.org/0000-0002-7365-7332

Clare Buckeridge − *Pfizer Worldwide Research, Development, and Medical, Cambridge, Massachusetts 02139, United States*

John M. Curto − *Pfizer Worldwide Research, Development, and Medical, Groton, Connecticut 06340, United States*

David R. Derksen − *Pfizer Worldwide Research, Development, and Medical, Groton, Connecticut 06340, United States*

João M. Dias − *Pfizer Worldwide Research, Development, and Medical, Groton, Connecticut 06340, United States*

Matthew C. Griffor − *Pfizer Worldwide Research, Development, and Medical, Groton, Connecticut 06340, United States*

Seungil Han − *Pfizer Worldwide Research, Development, and Medical, Groton, Connecticut 06340, United States*

V. Margaret Jackson − *Pfizer Worldwide Research, Development, and Medical, Cambridge, Massachusetts 02139, United States*

Margaret S. Landis − *Pfizer Worldwide Research, Development, and Medical, Cambridge, Massachusetts 02139, United States*

Daniel Lettiere − *Pfizer Worldwide Research, Development, and Medical, Groton, Connecticut 06340, United States*

Chris Limberakis − *Pfizer Worldwide Research, Development, and Medical, Groton, Connecticut 06340, United States;* orcid.org/0000-0003-2987-680X

Yuhang Liu − *Pfizer Worldwide Research, Development, and Medical, Groton, Connecticut 06340, United States*

Alan M. Mathiowetz − *Pfizer Worldwide Research, Development, and Medical, Cambridge, Massachusetts 02139, United States*

Jayesh C. Patel − *Sosei Heptares, Cambridge CB21 6DG, U.K.*

David W. Piotrowski − *Pfizer Worldwide Research, Development, and Medical, Groton, Connecticut 06340, United States;* orcid.org/0000-0002-4659-6300

David A. Price − *Pfizer Worldwide Research, Development, and Medical, Cambridge, Massachusetts 02139, United States*

Roger B. Ruggeri − *Pfizer Worldwide Research, Development, and Medical, Cambridge, Massachusetts 02139, United States;* orcid.org/0000-0001-9813-1882

David A. Tess − *Pfizer Worldwide Research, Development, and Medical, Cambridge, Massachusetts 02139, United States*

Complete contact information is available at: https://pubs.acs.org/10.1021/acs.jmedchem.1c01856

Author Contributions

Formulation or evolution of overarching research goals and aims: D.A.G., A.S.K., D.J.E., J.B.K., P.M.L., V.M.J., and J.-P.F. Data curation: J.B.K., D.R.D., P.M.L., and J.-P.F. Application of statistical and/or mathematical analyses: A.R.S., J.B.K., D.R.D., C.B., and J.-P.F. Acquisition of funding: V.M.J. Conducting the research and/or collecting data: D.A.G., A.S.K., A.M.M., C.L., S.W.B., A.R.S., S.H., D.J.E., M.C.G., J.B.K., D.R.D., J.M.D., V.M.J., J.M.C., C.B., R.B.R., D.L., J.-P.F., Y.L., D.A.T., M.S.L., and J.C.P. Project administration: M.S.L. and D.A.P. Provision of study resources, including animals and patients: V.M.J. and M.S.L. Implementation of the relevant software or computer programs: C.B. Oversight and leadership of the study planning and execution: D.A.G., A.R.S., S.H., D.J.E., J.B.K., P.M.L., J.M.D., V.M.J., C.B., D.L., J.-P.F., and M.S.L. Data verification and validation: A.S.K., S.W.B., A.R.S., D.W.P., M.C.G., J.B.K., D.R.D., P.M.L., C.B., J.-P.F., D.A.T., and M.S.L. Preparation of the data and graphical elements of the paper: D.A.G., A.S.K., C.L., D.W.P., D.J.E., J.B.K., D.R.D., P.M.L., J.M.D., C.B., J.-P.F., Y.L., and D.A.T. Preparation of the written elements of the paper: D.A.G., A.S.K., C.L., A.R.S., D.W.P., D.J.E., J.B.K., D.R.D., P.M.L., J.M.D., J.-P.F., and Y.L. Editing and review of the paper: D.A.G., A.S.K., A.M.M., C.L., S.W.B., A.R.S., D.W.P., S.H., D.J.E., M.C.G., J.B.K., D.R.D., P.M.L., J.M.D., C.B., R.B.R., D.L., J.M.C., J.-P.F., Y.L., M.S.L., and D.A.P.

Notes

The authors declare the following competing financial interest(s): A.S.K., A.M.M., M.C.G., J.M.D., C.B., C.L., S.W.B., D.L., P.M.L., D.R.D., J.M.C., J.-P.F., Y.L., A.R.S., D.A.T., D.W.P., S.H., M.S.L., and D.A.G. are employees and stockholders of Pfizer Inc. J.B.K., D.J.E., R.B.R., D.A.P., and V.M.J. are stockholders of Pfizer Inc. J.C.P. is an employee and stockholder of Sosei Heptares.

Upon request, and subject to review, Pfizer will provide the data that support the findings of this study. Subject to certain criteria, conditions, and exceptions, Pfizer may also provide access to the related individual deidentified participant data. See https://www.pfizer.com/science/clinical-trials/trial-data-and-results for more information.

■ ACKNOWLEDGMENTS

The authors thank the participants of the FIH study; T. P. Rolph, S. Liras, and M. J. Birnbaum for continued support of the oral GLP-1R agonist program; M. E. Flanagan for sharing expertise in medicinal chemistry; G. E. Aspnes, S. B. Coffey, E. L. Conn, A. Dion, M. S. Dowling, G. Ingle, W. Jiao, A. Shavnya, and L. Wei for compound synthesis and route design; J. N. Bradow, J. K. Smith, and X. Wang for analytical support; J. X. Kong, L. Rogers, J. J. Shah, and K. A. Stevens for the execution of *in vitro* activity assays; K. Schildknegt for overseeing radiosynthesis; B. L. Bernardo, S. Joaquim, N. Nammi, and A. H. Smith for execution of *in vivo* testing; D. Gates and K. N. Yip for compound formulation; H. Eng for execution of pharmacokinetics studies; K. F. Fennell for protein reagent generation; D. N. Gorman and A. Bannerjee for statistical support; S. Farenden and E. Madigan for coordinating pharmaceutical science activities; M. Popovitz, M. C. Sanford, and S. Uppal for clinical study execution; M. J. Vorko for project management; X. Qiu, J. Pandit, and A. H. Varghese for supporting the Pfizer membrane protein cryo-EM initiative; Terry Kenakin for statistical analysis of the signaling bias data; and Stacey Southall, Mathieu Rappas, and Cedric Fiez-Vandal of Sosei Heptares for producing a stabilized GLP-1R engineered using their proprietary StaR technology to enable our structural studies. This study was sponsored by Pfizer Inc. Medical writing support, under the direction of the authors, was provided by Eric Comeau, Ph.D., of CMC Connect, McCann Health Medical Communications, and was funded by Pfizer Inc. (New York, NY), in accordance with Good Publication Practice (GPP3) guidelines (*Ann. Intern. Med.* **2015**, *163*, 461−464).

■ ABBREVIATIONS USED

AE, adverse event; AUC, area under the plasma concentration versus time curve; βArr, β-arrestin; βArr1, β-arrestin-1; βArr2, β-arrestin-2; BETP, 4-[3-(benzyloxy)phenyl]-2-ethylsulfinyl-6-(trifluoromethyl)pyrimidine; cAMP, cyclic adenosine monophosphate; CHO, Chinese hamster ovary; CL_{int}, intrinsic clearance; CL_p, high plasma clearance; C_{max}, maximal plasma concentration; cryo-EM, cryogenic electron microscope; CS, candidate selection; ECD, extracellular domain; EC_{50}, half-maximal effective concentration; E_{max}, maximal effect; FAP, fluorogen-activated protein; Gαs, guanine nucleotide-binding α stimulatory subunit; GFP, green fluorescent protein; GLP-1R, glucagon-like peptide-1 receptor; GPCR, G protein-coupled receptor; HbA1c, glycated hemoglobin; HEK, human embryonic kidney; hERG, human ether-a-go-go-related gene; HLM, human liver microsomes; HPLC, high-performance liquid chromatography; HTS, high-throughput screening; IR, immediate release; iv, intravenous; IVGTT, intravenous glucose tolerance test; K_i, inhibition constant; NMR, nuclear magnetic resonance; PAM, positive allosteric modulator; PDB, Protein Data Bank; po, oral; RO, receptor occupancy; S, serine; SA, screening assay; SAR, structure−activity relationship; SEM, standard error of the mean; $t_{1/2}$, elimination half-life; T2DM, type 2 diabetes mellitus; T_{max}, median time to reach C_{max}; W, tryptophan

■ ADDITIONAL NOTE

[a]Compound **15** safety risk! Differential scanning calorimetry has identified a significant exotherm for compound **15** (>1500 J/g) with an initiation temperature of 235 °C.

■ REFERENCES

(1) Drucker, D. J.; Mojsov, S.; Habener, J. F. Cell-specific post-translational processing of preproglucagon expressed from a metallothionein-glucagon fusion gene. *J. Biol. Chem.* **1986**, *261*, 9637−9643.

(2) Orskov, C.; Holst, J. J.; Knuhtsen, S.; Baldissera, F. G.; Poulsen, S. S.; Nielsen, O. V. Glucagon-like peptides GLP-1 and GLP-2, predicted products of the glucagon gene, are secreted separately from pig small intestine but not pancreas. *Endocrinology* **1986**, *119*, 1467−1475.

(3) Orskov, C.; Rabenhøj, L.; Wettergren, A.; Kofod, H.; Holst, J. J. Tissue and plasma concentrations of amidated and glycine-extended glucagon-like peptide I in humans. *Diabetes* **1994**, *43*, 535−539.

(4) Kreymann, B.; Williams, G.; Ghatei, M. A.; Bloom, S. R. Glucagon-like peptide-1 7−36: a physiological incretin in man. *Lancet* **1987**, *330*, 1300−1304.

(5) Nauck, M. A.; Niedereichholz, U.; Ettler, R.; Holst, J. J.; Orskov, C.; Ritzel, R.; Schmiegel, W. H. Glucagon-like peptide 1 inhibition of gastric emptying outweighs its insulinotropic effects in healthy humans. *Am. J. Physiol.* **1997**, *273*, e981−e988.
(6) Drucker, D. J. Mechanisms of action and therapeutic application of gucagon-like peptide-1. *Cell Metab.* **2018**, *27*, 740−756.
(7) Burcelin, R.; Gourdy, P. Harnessing glucagon-like peptide-1 receptor agonists for the pharmacological treatment of overweight and obesity. *Obes. Rev.* **2017**, *18*, 86−98.
(8) Nauck, M. Incretin therapies: highlighting common features and differences in the modes of action of glucagon-like peptide-1 receptor agonists and dipeptidyl peptidase-4 inhibitors. *Diabetes Obes. Metab.* **2016**, *18*, 203−216.
(9) Novo Nordisk A/S. *WEGOVY (semaglutide) prescribing information*. https://www.novo-pi.com/wegovy.pdf (accessed 2021-08-21).
(10) Novo Nordisk A/S. *SAXENDA (liraglutide) prescribing information*. https://www.novo-pi.com/saxenda.pdf (accessed 2021-08-21).
(11) Dalsgaard, N. B.; Brønden, A.; Vilsbøll, T.; Knop, F. K. Cardiovascular safety and benefits of GLP-1 receptor agonists. *Expert Opin. Drug Saf.* **2017**, *16*, 351−363.
(12) Dibonaventura, M. D.; Wagner, J. S.; Girman, C. J.; Brodovicz, K.; Zhang, Q.; Qiu, Y.; Sri-Ram, P.; Radican, L. Multinational internet-based survey of patient preference for newer oral or injectable type 2 diabetes medication. *Patient Preference Adherence* **2010**, *4*, 397−406.
(13) Novo Nordisk A/S. *RYBELSUS (semaglutide) prescribing information*. https://www.novo-pi.com/rybelsus.pdf (accessed 2021-08-21).
(14) Granhall, C.; Donsmark, M.; Blicher, T. M.; Golor, G.; Søndergaard, F. L.; Thomsen, M.; Bækdal, T. A. Safety and pharmacokinetics of single and multiple ascending doses of the novel oral human GLP-1 analogue, oral semaglutide, in healthy subjects and subjects with type 2 diabetes. *Clin. Pharmacokinet.* **2019**, *58*, 781−791.
(15) de Graaf, C.; Song, G.; Cao, C.; Zhao, Q.; Wang, M. W.; Wu, B.; Stevens, R. C. Extending the structural view of class B GPCRs. *Trends Biochem. Sci.* **2017**, *42*, 946−960.
(16) Edmonds, D. J.; Price, D. A. Oral GLP-1 modulators for the treatment of diabetes. *Annu. Rep. Med. Chem.* **2013**, *48*, 119−130.
(17) Willard, F. S.; Bueno, A. B.; Sloop, K. W. Small molecule drug discovery at the glucagon-like peptide-1 receptor. *Exp. Diabetes Res.* **2012**, *2012*, 709893.
(18) Chugai Pharmaceutical Co. Ltd. Pyrazolopyridine derivative having GLP-1 receptor agonist effect. WO 2018056453, 2018.
(19) Thorens, B. Expression cloning of the pancreatic beta cell receptor for the gluco-incretin hormone glucagon-like peptide 1. *Proc. Natl. Acad. Sci. U.S.A.* **1992**, *89*, 8641−8645.
(20) Fletcher, M. M.; Halls, M. L.; Christopoulos, A.; Sexton, P. M.; Wootten, D. The complexity of signalling mediated by the glucagon-like peptide-1 receptor. *Biochem. Soc. Trans.* **2016**, *44*, 582−588.
(21) Jones, B.; Buenaventura, T.; Kanda, N.; Chabosseau, P.; Owen, B. M.; Scott, R.; Goldin, R.; Angkathunyakul, N.; Corrêa, I. R., Jr.; Bosco, D.; Johnson, P. R.; Piemonti, L.; Marchetti, P.; Shapiro, A. M. J.; Cochran, B. J.; Hanyaloglu, A. C.; Inoue, A.; Tan, T.; Rutter, G. A.; Tomas, A.; Bloom, S. R. Targeting GLP-1 receptor trafficking to improve agonist efficacy. *Nat. Commun.* **2018**, *9*, 1602.
(22) Fortin, J. P.; Zhu, Y.; Choi, C.; Beinborn, M.; Nitabach, M. N.; Kopin, A. S. Membrane-tethered ligands are effective probes for exploring class B1 G protein-coupled receptor function. *Proc. Natl. Acad. Sci. U.S.A.* **2009**, *106*, 8049−8054.
(23) Al-Sabah, S.; Al-Fulaij, M.; Shaaban, G.; Ahmed, H. A.; Mann, R. J.; Donnelly, D.; Bünemann, M.; Krasel, C. The GIP receptor displays higher basal activity than the GLP-1 receptor but does not recruit GRK2 or arrestin3 effectively. *PLoS One* **2014**, *9*, e106890.
(24) Kobilka, B. K.; Deupi, X. Conformational complexity of G-protein-coupled receptors. *Trends Pharmacol. Sci.* **2007**, *28*, 397−406.
(25) Wootten, D.; Savage, E. E.; Valant, C.; May, L. T.; Sloop, K. W.; Ficorilli, J.; Showalter, A. D.; Willard, F. S.; Christopoulos, A.; Sexton, P. M. Allosteric modulation of endogenous metabolites as an avenue for drug discovery. *Mol. Pharmacol.* **2012**, *82*, 281−290.
(26) Willard, F. S.; Wootten, D.; Showalter, A. D.; Savage, E. E.; Ficorilli, J.; Farb, T. B.; Bokvist, K.; Alsina-Fernandez, J.; Furness, S. G.; Christopoulos, A.; Sexton, P. M.; Sloop, K. W. Small molecule allosteric modulation of the glucagon-like peptide-1 receptor enhances the insulinotropic effect of oxyntomodulin. *Mol. Pharmacol.* **2012**, *82*, 1066−1073.
(27) Nolte, W. M.; Fortin, J. P.; Stevens, B. D.; Aspnes, G. E.; Griffith, D. A.; Hoth, L. R.; Ruggeri, R. B.; Mathiowetz, A. M.; Limberakis, C.; Hepworth, D.; Carpino, P. A. A potentiator of orthosteric ligand activity at GLP-1R acts via covalent modification. *Nat. Chem. Biol.* **2014**, *10*, 629−631.
(28) Chen, D.; Liao, J.; Li, N.; Zhou, C.; Liu, Q.; Wang, G.; Zhang, R.; Zhang, S.; Lin, L.; Chen, K.; Xie, X.; Nan, F.; Young, A. A.; Wang, M. W. A nonpeptidic agonist of glucagon-like peptide 1 receptors with efficacy in diabetic db/db mice. *Proc. Natl. Acad. Sci. U.S.A.* **2007**, *104*, 943−948.
(29) Wootten, D.; Savage, E. E.; Willard, F. S.; Bueno, A. B.; Sloop, K. W.; Christopoulos, A.; Sexton, P. M. Differential activation and modulation of the glucagon-like peptide-1 receptor by small molecule ligands. *Mol. Pharmacol.* **2013**, *83*, 822−834.
(30) Hoang, H. N.; Song, K.; Hill, T. A.; Derksen, D. R.; Edmonds, D. J.; Kok, W. M.; Limberakis, C.; Liras, S.; Loria, P. M.; Mascitti, V.; Mathiowetz, A. M.; Mitchell, J. M.; Piotrowski, D. W.; Price, D. A.; Stanton, R. V.; Suen, J. Y.; Withka, J. M.; Griffith, D. A.; Fairlie, D. P. Short hydrophobic peptides with cyclic constraints are potent glucagon-like peptide-1 receptor (GLP-1R) agonists. *J. Med. Chem.* **2015**, *58*, 4080−4085.
(31) Aspnes, G. E.; Bagley, S. W.; Conn, E. L.; Curto, J. M.; Edmonds, D. J.; Flanagan, M. E.; Futatsugi, K.; Griffith, D. A.; Huard, K.; Limberakis, C.; Mathiowetz, A. M.; Piotrowski, D. W.; Ruggeri, R. B. GLP-1 Agonists and Uses Thereof. WO 2019/239371, 2019.
(32) Aspnes, G. E.; Bagley, S. W.; Curto, J. M.; Dowling, M. S.; Edmonds, D. J.; Flanagan, M. E.; Futatsugi, K.; Griffith, D. A.; Huard, K.; Ingle, G.; Jiao, W.; Limberakis, C.; Mathiowetz, A. M.; Piotrowski, D. W.; Ruggeri, R. B. GLP-1 receptor agonists and uses thereof. WO 2018/109607, 2018.
(33) Brameld, K. A.; Kuhn, B.; Reuter, D. C.; Stahl, M. Small molecule conformational preferences derived from crystal structure data. A medicinal chemistry focused analysis. *J. Chem. Inf. Model.* **2008**, *48*, 1−24.
(34) Recanatini, M.; Poluzzi, E.; Masetti, M.; Cavalli, A.; De Ponti, F. QT prolongation through hERG K^+ channel blockade: current knowledge and strategies for the early prediction during drug development. *Med. Res. Rev.* **2005**, *25*, 133−166.
(35) Johnson, T. W.; Gallego, R. A.; Edwards, M. P. Lipophilic efficiency as an important metric in drug design. *J. Med. Chem.* **2018**, *61*, 6401−6420.
(36) Lombardo, F.; Shalaeva, M. Y.; Tupper, K. A.; Gao, F. $ElogD_{oct}$: a tool for lipophilicity determination in drug discovery. 2. Basic and neutral compounds. *J. Med. Chem.* **2001**, *44*, 2490−2497.
(37) Stopher, D.; McClean, S. An improved method for the determination of distribution coefficients. *J. Pharm. Pharmacol.* **2011**, *42*, 144.
(38) Obach, R. S. Predicting clearance in humans from in vitro data. *Curr. Top. Med. Chem.* **2011**, *11*, 334−339.
(39) Kenakin, T. Predicting therapeutic value in the lead optimization phase of drug discovery. *Nat. Rev. Drug Discovery* **2003**, *2*, 429−438.
(40) Knudsen, L. B.; Hastrup, S.; Underwood, C. R.; Wulff, B. S.; Fleckner, J. Functional importance of GLP-1 receptor species and expression levels in cell lines. *Regul. Pept.* **2012**, *175*, 21−29.
(41) Kenakin, T. A scale of agonism and allosteric modulation for assessment of selectivity, bias, and receptor mutation. *Mol. Pharmacol.* **2017**, *92*, 414−424.

https://doi.org/10.1021/acs.jmedchem.1c01856
J. Med. Chem. 2022, 65, 8208−8226

(42) Zhang, X.; Belousoff, M. J.; Zhao, P.; Kooistra, A. J.; Truong, T. T.; Ang, S. Y.; Underwood, C. R.; Egebjerg, T.; Šenel, P.; Stewart, G. D.; Liang, Y. L.; Glukhova, A.; Venugopal, H.; Christopoulos, A.; Furness, S. G. B.; Miller, L. J.; Reedtz-Runge, S.; Langmead, C. J.; Gloriam, D. E.; Danev, R.; Sexton, P. M.; Wootten, D. Differential GLP-1R binding and activation by peptide and non-peptide agonists. *Mol. Cell* **2020**, *80*, 485−500.
(43) Liang, Y. L.; Khoshouei, M.; Glukhova, A.; Furness, S. G. B.; Zhao, P.; Clydesdale, L.; Koole, C.; Truong, T. T.; Thal, D. M.; Lei, S.; Radjainia, M.; Danev, R.; Baumeister, W.; Wang, M. W.; Miller, L. J.; Christopoulos, A.; Sexton, P. M.; Wootten, D. Phase-plate cryo-EM structure of a biased agonist-bound human GLP-1 receptor-Gs complex. *Nature* **2018**, *555*, 121−125.
(44) Pettersen, E. F.; Goddard, T. D.; Huang, C. C.; Couch, G. S.; Greenblatt, D. M.; Meng, E. C.; Ferrin, T. E. UCSF Chimera—a visualization system for exploratory research and analysis. *J. Comput. Chem.* **2004**, *25*, 1605−1612.
(45) Tibaduiza, E. C.; Chen, C.; Beinborn, M. A small molecule ligand of the glucagon-like peptide 1 receptor targets its amino-terminal hormone binding domain. *J. Biol. Chem.* **2001**, *276*, 37787−37793.
(46) Dods, R. L.; Donnelly, D. The peptide agonist-binding site of the glucagon-like peptide-1 (GLP-1) receptor based on site-directed mutagenesis and knowledge-based modelling. *Biosci. Rep.* **2016**, *36*, e00285.
(47) Zhang, Y.; Sun, B.; Feng, D.; Hu, H.; Chu, M.; Qu, Q.; Tarrasch, J. T.; Li, S.; Sun Kobilka, T.; Kobilka, B. K.; Skiniotis, G. Cryo-EM structure of the activated GLP-1 receptor in complex with a G protein. *Nature* **2017**, *546*, 248−253.
(48) Hennen, S.; Kodra, J. T.; Soroka, V.; Krogh, B. O.; Wu, X.; Kaastrup, P.; Ørskov, C.; Rønn, S. G.; Schluckebier, G.; Barbateskovic, S.; Gandhi, P. S.; Reedtz-Runge, S. Structural insight into antibody-mediated antagonism of the glucagon-like peptide-1 receptor. *Sci. Rep.* **2016**, *6*, 26236.
(49) Pyke, C.; Heller, R. S.; Kirk, R. K.; Ørskov, C.; Reedtz-Runge, S.; Kaastrup, P.; Hvelplund, A.; Bardram, L.; Calatayud, D.; Knudsen, L. B. GLP-1 receptor localization in monkey and human tissue: novel distribution revealed with extensively validated monoclonal antibody. *Endocrinology* **2014**, *155*, 1280−1290.
(50) Kawai, T.; Sun, B.; Yoshino, H.; Feng, D.; Suzuki, Y.; Fukazawa, M.; Nagao, S.; Wainscott, D. B.; Showalter, A. D.; Droz, B. A.; Kobilka, T. S.; Coghlan, M. P.; Willard, F. S.; Kawabe, Y.; Kobilka, B. K.; Sloop, K. W. Structural basis for GLP-1 receptor activation by LY3502970, an orally active nonpeptide agonist. *Proc. Natl. Acad. Sci. U.S.A.* **2020**, *117*, 29959−29967.
(51) Zhao, P.; Liang, Y. L.; Belousoff, M. J.; Deganutti, G.; Fletcher, M. M.; Willard, F. S.; Bell, M. G.; Christe, M. E.; Sloop, K. W.; Inoue, A.; Truong, T. T.; Clydesdale, L.; Furness, S. G. B.; Christopoulos, A.; Wang, M. W.; Miller, L. J.; Reynolds, C. A.; Danev, R.; Sexton, P. M.; Wootten, D. Activation of the GLP-1 receptor by a non-peptidic agonist. *Nature* **2020**, *577*, 432−436.
(52) Saxena, A. R.; Gorman, D. N.; Esquejo, R. M.; Bergman, A.; Chidsey, K.; Buckeridge, C.; Griffith, D. A.; Kim, A. M. Danuglipron (PF-06882961) in type 2 diabetes: a randomized, placebo-controlled, multiple ascending-dose phase 1 trial. *Nat. Med.* **2021**, *27*, 1079−1087.
(53) Pfizer Inc. GLP-1 receptor agonists and uses thereof. WO 2018109607, 2018.

https://doi.org/10.1021/acs.jmedchem.1c01856
J. Med. Chem. 2022, 65, 8208−8226